Water resistant electrospun nanofibers composed of nanocellulose and conducting polymer

Åbo Akademi University

Faculty of Science and Engineering

Jose Antonio Wrzosek Cabrera

Master's programme in Excellence in Analytical Chemistry

Degree project in Analytical chemistry, 30 credits

Supervisor: Rose-Marie Latonen (Åbo Akademi University)

Cosupervisor(s): Tarmo Tamm (University of Tartu)

May, 2019

Abstract

Nanofibers of novel polymer compositions containing cellulose nanofibrils and the conducting polymer poly(3,4-ethylenedioxythiophene) doped with polystyrene sulfonate (PEDOT:PSS) were prepared via electrospinning and characterized regarding their morphology, water resistivity and electrical activity. Poly(ethylene oxide) (PEO) was used to support the electrospinning process and poly(ethylene glycol) diglycidyl ether as a cross-linking agent to induce water resistivity to the nanofibers.

The influence of different dispersion compositions, pumping rates and applied potentials on the electrospinning process were studied, and the best parameters were chosen based on the morphology and electroactivity of the nanofibers.

Scanning electron microscopy (SEM) was used to study the morphology of the electrospun nanofibers and Energy Dispersive X-ray Analysis (EDXA) to determine the C/S ratio of the nanofibers made with different dispersion compositions.

The nanofibers with the most uniform morphologies were studied with cyclic voltammetry in order to find out their electrical activity. All nanofibers tested exhibited a capacitor-like behavior.

The stability of the nanofibers in water was also studied by measuring the long-term electrical activity with cyclic voltammetry. The best compositions were stable for up to two months with little to no lessening of their charging capacity. Infrared spectroscopy was used to study the changes in the molecular structure of the nanofibers before and after contact with water. It was observed that PEO dissolved in water but the PEDOT:PSS/CNF structure remained. Nanofiber diameter appeared to increase from approximately 200 nm to 350 nm as shown by SEM.

Keywords: Electrospinning, cyclic voltammetry, nanofibers, nanocellulose, poly(ethylene oxide), poly(3,4-ethylenedioxythiophene), poly(ethylene glycol) diglycidyl ether.

Preface

The following thesis work was performed at the Laboratory of Analytical chemistry at Åbo Akademi University, as part of the work required to obtain the M.Sc. degree in the Erasmus Mundus joint program “Excellence in Analytical Chemistry”, EACH.

I wish to thank my supervisors, Docent Rose-Marie Latonen and Dr. Tarmo Tamm for their valuable insight and suggestions during the writing of this work.

Special thanks also to all my friends in Turku, who made the writing of this thesis bearable. Without you guys, I would have crashed a long time ago.

And finally, to my family, for their invaluable support and for making me feel at home even though I am 9000 km away.

Table of contents

List of abbreviations

ATR	Attenuated Total Reflectance
BC, BNC	Bacterial cellulose
BSEs	Backscattered electrons
CNC	Cellulose nanocrystals
CNF	Cellulose nanofibrils
CV	Cyclic voltammetry
EDXA	Energy-dispersive X-ray analysis
EIS	Electrospun fibers
FT-IR	Fourier transform infrared spectroscopy
GC	Glassy carbon
GPa	Giga Pascal
IR	Infrared radiation
ITO	Indium tin oxide
KCl	Potassium chloride
PANI	Polyaniline
PEs	Primary electrons
PEGDE	Poly(ethylene glycol) diglycidyl ether
PEDOT	Poly(3,4-ethylenedioxythiophene)
PEDOT:PSS	Poly(3,4-ethylenedioxythiophene) doped with PSS
PEO	Poly(ethylene oxide)
PPy	Polypyrrole
PSS	Polystyrene sulfonate
SEs	Secondary electrons
SEM	Scanning electron microscopy

1. Introduction

Nanofibers are an interesting group of materials which have shown increasing interest due to their suitability for many different applications ranging from water treatment[1], batteries[2,4], improving sensors' detection limits[3], catalyst applications[5], wound healing[6] and even brain tumor therapy[7]. One way to produce nanofibers is by electrospinning, an exciting technique in which a high electrical field is applied over a liquid polymer solution in order to generate an excess in charge across the polymer solution, which will propel the solution based on electrical repulsion forces, towards a grounded collector plate[8,9].

Nanofibers present characteristics that set them apart from macrofibers, such as high porosity, high surface-to-volume ratio and the ability to control fiber composition[8]. These characteristics allow for tailoring of fibers for use in specific applications, such as conductive fibers[10] and films[11] for solar cells[12,13] and fibers for tissue engineering[14]. Due to the versatility of the fibers obtained via electrospinning, different polymer compositions have been studied, ranging from SiO_2-cellulose acetate[15] to poly(ε-caprolactone)/nanocellulose[16] to conductive polymers, such as poly(3,4-ethylenedioxythiophene) (PEDOT)[11], and even natural organic polymers, such as cellulose[13].

Cellulose is the most abundant natural polymer[17,18,19], and has attracted a lot of attention from the scientific community due to its many possible applications, which include, but are not limited to, coating of biomolecules[20], scaffolds for bone tissue engineering[21], supercapacitors[22] and as nanocellulose in printed electronics[23]. Nanocellulose is a term that has been assigned to cellulose particles ranging in the nano-scale[23]. It can be classified as cellulose nanocrystals (CNC), cellulose nanofibrils (CNF) or bacterial cellulose (BC)[18,23], depending on the way it has been prepared. Nanocellulose has attracted a lot of attention due to it being environmentally friendly[23], abundant[18], biocompatible[6,7], possessing high mechanical strength[24] and stiffness[24], making it an interesting research material in the energy storage and electrode development fields in and the health care sector.

Conducting polymers are macromolecules that exhibit electrical activity by means of rearrangement of π-electrons[25] along a conjugated backbone. Among the most studied conducting polymers, PEDOT has gained a lot of attention due to its unique properties such as low band gap[10,11], high electrical conductivity[11, 26], biocompatibility[26] low oxidation potential[10,11] and good stability in the oxidized state[11], which makes it an interesting material for diverse applications, such as synthetic muscles[26], sensors[11,27] and supercapacitors[26,28].

The aim of this thesis works was to obtain nanofibers from a polymer dispersion containing CNF, poly(ethylene oxide) (PEO), PEDOT and poly(ethylene glycol) diglycidyl ether (PEGDE) through electrospinning. Fiber properties such as uniform morphology, good charging capacity and good stability in water, as well as to find electrospinning conditions allowing for these characteristics were sought for.

2. Theoretical part

2.1. Materials and methods

2.1.1. Nanofibers and electrospinning

A nanofiber is any type of fiber with a diameter lower than 100 nm[29]. Possessing interesting characteristics, such as high surface area to volume ratio[8,30] and superior mechanical performance[30], these materials have attracted attention from the scientific community due to their vast array of possible uses. Several methods, such as electrospinning[8,9], solution blow spinning[31], forcespinning™[,32], drawspinning[33], molecular self-assembly[34] and template synthesis[35] have been developed in order to manufacture nanofibers[30], each with their own specific benefits and drawbacks. From these methods, electrospinning stands out as a reliable method showing possibility to form reproducible fiber diameters, as well as versatility in the type of materials that can be turned into nanofibers[8,30].

Electrospinning is a technique based on the application of a high electric potential to a polymer solution, in order to alter the surface properties of the solution, and eject it, due to charge repulsion, from its container, usually a syringe with a needle, towards a grounded collector plate. The difference in electric potential between the needle and the collector plate will distort the polymer solution into a cone, known as Taylor cone[36]. After the Taylor cone is formed, the polymer solution will experience a stretching while it is attracted to the collector plate, leading to the formation of a very thin thread. The basic setup of an electrospinning instrument is depicted in Fig. 1.

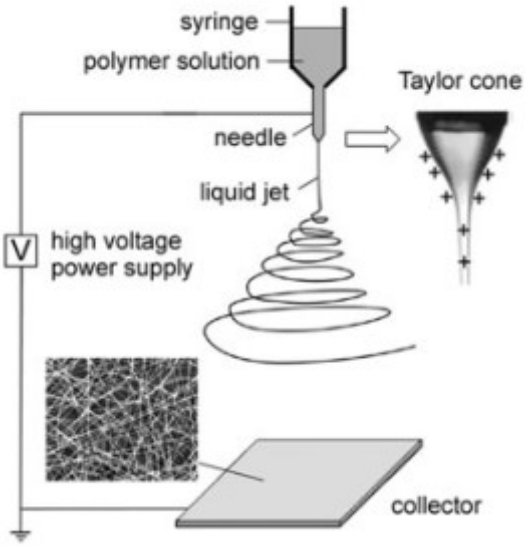

Fig. 1 Basic setup of an electrospinning instrument. Taken from Li D. & Xia Y., Electrospinning of Nanofibers: Reinventing the wheel?, 2004.

According to Bhardwaj and Kundu[8], the parameters which affect the quality and morphology of the fibers obtained with this process can be divided into two main groups: parameters concerning the polymer solution, such as viscosity and polymer concentration, and parameters concerning the electrospinning process, such as distance from the needle tip to the collector plate, potential applied and pumping rate. A lot of research has been done in order to better comprehend how the characteristics

of the polymer solution utilized during the electrospinning process impact the quality of the nanofibers. From the data obtained, some conclusions can be drawn. Jian et al.[37] observed that the viscosity of the solution has an impact on the presence of bead-like structures suggesting that the higher the viscosity of the solution, the less bead-like structures will be present on the nanofiber structure. The same behavior was also reported by Huang et al.[38], who additionally observed that a slow pumping rate (below 100 µl/min) promotes the formation of these structures. Kim et al.[39], observed that by controlling the ionic strength of the polymer solution, one can affect the fiber diameter and electric conductivity of the fibers, concluding that with a higher ionic strength, the diameter of the fibers increases. Similarly, Son et al.[40] reported an increase in PEO-nanofibers' diameter due to an increase in the PEO concentration of the polymer solution.

Equally, the electrospinning process parameters have shown to affect the morphology of the spun nanofibers. Demir et al.[41] observed that with higher concentrations of the polymer a higher applied voltage is required in order to start the formation of the Taylor cone. Regarding the distance from the needle tip to the collector plate, Zhao et al.[42] reported that no visible differences in fiber morphology other than small differences in fiber diameters were observed besides the distance was changed from 10 to 20 cm suggesting that distance may be an important factor to obtain thin threads.

From the research done over the many different parameters that influence the morphology of the obtained fibers, it can be concluded that specific conditions must be investigated based on the polymer composition that is being studied, since the properties of the fibers rely heavily on their morphology[43].

2.1.2. Nanocellulose

Cellulose, a polymer composed of glucose units, is one of the most abundant natural and renewable polymers[17,18,19]. It is obtained mainly from plants, since it is a part of their cellular wall, but it has been observed that bacterial organisms, such as *Acetobacter xylinum* can also produce cellulose[44]. Fig. 2 showcases the structure of cellulose.

It has been observed that when cellulose fibers are brought down to the nanoscale level, cellulose properties change radically[45] mainly its mechanical properties, going from elastic modulus values of 5-128 GPa for cellulose to 130-145 GPa for nanocellulose[46]. Due to this, the term nanocellulose was coined in order to indicate the scale of the material.

Nanocellulose can be divided into three groups: bacterial cellulose (BC, BNC) which is extracted from microorganisms, cellulose nanofibrils (CNF) obtained from delamination of plant-origin cellulose and cellulose nanocrystals (CNC) which are isolated from cellulose by chemical hydrolysis or oxidation[18,47]. This division is done based on the procedure utilized to obtain the nanocellulose. It has been said that nanocellulose has potential for utilization as reinforcement in polymer compositions, due to the high strength and stiffness nanocellulose possess[48].

CNF is commonly obtained from cellulosic fibers by chemical[18], mechanical[18,47] or a combination of both methods. When CNF is dissolved in water, a gel is obtained, with

concentrations as low as 0.125wt% CNF[49]. Research on this type of material is being focused mainly in the energy field, such as solar cells, supercapacitors and lithium ion batteries[47,48,50], printed electronics[23] and water treatment technologies[51]. It has been observed that addition of CNF to natural rubber slightly influences the electrical conductivity of a natural rubber/CNF nanocomposite[52].

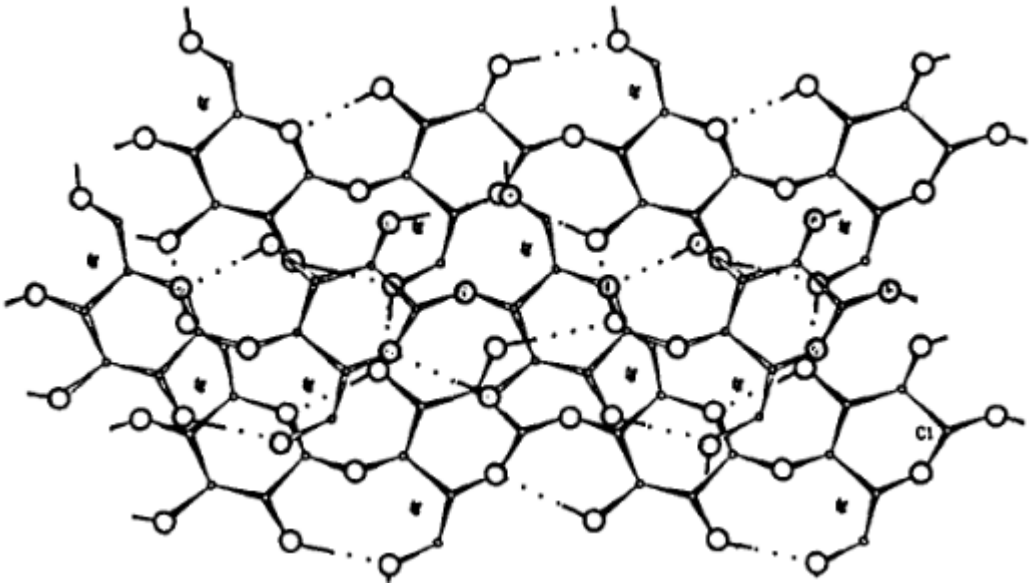

Fig. 2 Structure of cellulose. Taken from Aabloo et al., Packing energy calculations on the crystalline structure of cellulose I, 1995

Cellulose is insoluble in water[53], but it presents a high level of hygroscopicity[54]. It has also been observed that cellulose fibers in water can swell up to 20 to 35%[54]. This allows good compatibility with polymers that are water soluble, such as PEO. Nanocellulose has been used to improve the mechanical properties of a variety of fossil-based and bio-based polymers such as acrylate latex, carboxymethylcellulose, polysulfone, epoxides and thermoplastic starch, among others[46], but complications arose due to the moisture sensitivity of nanocellulose, and its incompatibility with lipophilic polymers[55]. When electrospun, nanocellulose has been shown to improve the mechanical properties of the composites it is spun into[17]. Fortunato et al.[56] electrospun CNF with PEO, observing that the viscosity and electrical conductivity of PEO increased with the addition of CNF, as well as an improvement of the mechanical properties of PEO/CNF fibers compared to PEO.

2.1.3. Conducting polymers

Conducting polymers are organic materials with tuneable electrical conductivity, that allow movement of electrons through them thanks to the presence of alternating single and double bonds in their conjugated structure. Some characteristics of conducting polymers are high electrical conductivity and light weight[26]. Among the most studied conducting polymers are PEDOT:PSS[10,11,57], polyaniline (PANI)[58,59,60] and polypyrrole (PPy)[61,62,63].

Conducting polymers, in their neutral state, present characteristics which do not mirror those of electrically conducting materials. However, once there is a deficit or excess

of electrons in the polymer structure, due to the presence of electron-deficient or electron-rich species, known as a dopant, the polymer will become conducting[64].

PEDOT has a unique set of electrical properties, such as low oxidation potential and high conductivity, in addition to high stability which makes it an interesting material that has received a lot of attention in recent years[11,65].

2.2. Characterization techniques

2.2.1. Scanning electron microscopy

Scanning electron microscopy (SEM) is an imaging technique which allows the visualization of the topography of materials by irradiating an electron beam over the sample. A detector picks up the secondary electrons or backscattered electrons that are generated by the interaction of the electrons in the electron beam with the components in the sample[66].

The principle of operation of this technique revolves around the generation of a beam of electrons which is directed towards the sample. Due to this, SEM imaging requires a vacuum, to avoid the scattering of primary electrons (PE) prior to impacting with the sample. Upon impact, the electrons released by the sample can be classified into secondary electrons or backscattered electrons[66].

If the PE loses energy when impacting with the sample, the electrons obtained from this interaction are called secondary electrons (SEs). These electrons are contained on the outer shell of the atoms present in the surface of the sample and don't require a huge amount of energy to be released. These electrons are the ones responsible for the topography observed in SEM images. If the PE doesn't lose energy when they impact with the sample, they can penetrate deeper into the material, and cause the release of the so-called backscattered electrons (BSEs)[66,67].

2.2.2. Energy-dispersive X-ray spectroscopy

X-ray analysis are based on the same principle as SEM. The main difference between this technique and SEM is the information obtained and how the signal is generated.

When a PE impacts on an atom, it can release either an outer shell electron or an inner shell electron. After a PE has knocked the electron out of the energy shell, the atom enters a high-energy state, which will persist for a moment, and then the atom will start to relax by moving one electron from one of its energy shells to fill the void caused by the PE beam. If the electron in the sample has been knocked out from an inner electronic shell, the relaxation process will release a huge amount of energy, which will be detected as X-rays[68,69]. Fig. 3 illustrates the possible paths the relaxation process can undergo from the high-energy state to the relaxed state. The X-rays generated are always element specific, which makes EDXA a characterization technique that can be coupled with SEM to obtain information about the elemental distribution of the components in a sample.

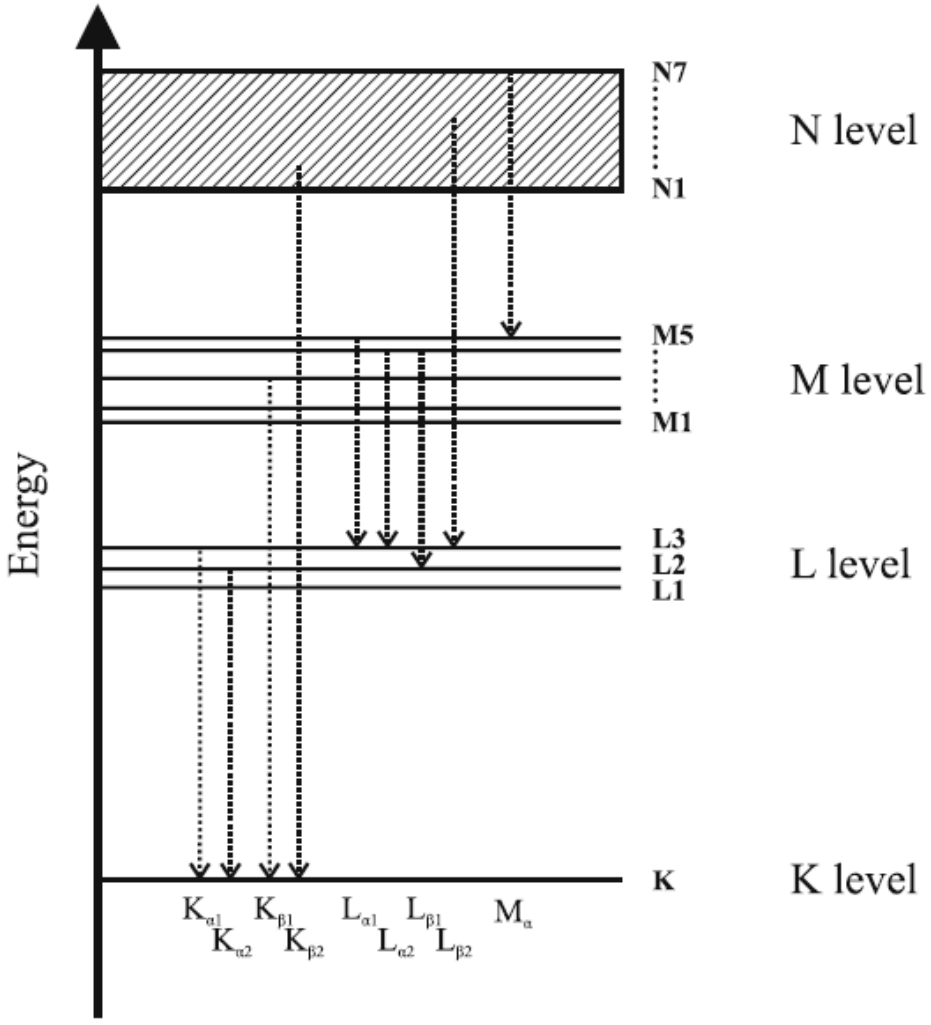

Fig. 3 Energy levels and possible electron transitions. Taken from Michler, G.H., Electron Microscopy of Polymers, 2008.

2.2.3. Cyclic voltammetry

Cyclic voltammetry is an amperometric technique which consists of recording the current occurring on top of the working electrode due to a Faradaic process as a function of the applied potential[70]. The measurement setup is based upon the three-electrode cell system, which is depicted in Fig. 4. The potential is controlled between the counter electrode and the reference electrode, and the change in current between the working electrode and the counter electrode is registered.

A potential sweep is started from E_1 to E_2 with a know sweep rate. Upon reaching E_2 the potential is reversed back to E_1 and upon reaching E_1, the potential can be reversed back to E_2, continued to a new E value or stopped. The voltammogram obtained from this potential scanning can then be used to obtain a vast amount of information regarding the electrochemical process that takes place on the working electrode.

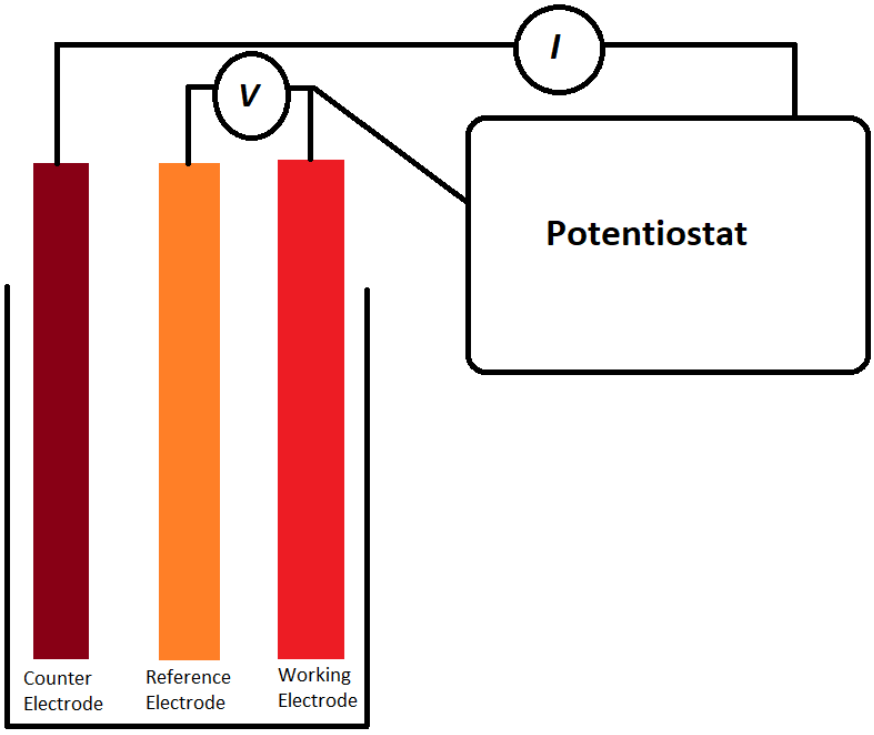

Fig. 4 3-electrode electrochemical cell used for cyclic voltammetric measurements

2.2.4. Fourier-transform Infrared spectroscopy

Infrared spectroscopy in based on the interaction of infrared radiation with matter. Infrared radiation (IR) is characterized by possessing a high wavelength number with a low energy. When IR is shined upon a molecule, it will cause the molecule to vibrate, if dipoles are present in its structure. The dipole must be asymmetrical in order to be able to be detected in an IR-spectrum[71]. The vibrational bands that the molecules absorb are highly characteristic and allow for the identification of certain molecular groups in the structure of the material that is being studied.

Attenuated Total Reflectance (ATR) is a sampling technique for FT-IR. It is based on the principle that when light goes from a medium with a high refractive index, i.e. a crystal, to a medium with low refractive index i.e. a sample, some of the light waves are going to be reflected back, a phenomenon called “total internal reflection”[72]. In this state, some light will scape from the material with the high refractive index towards the low refractive one, in the form of waves, called evanescent wave[72]. This residual radiation will then interact with the sample and be reflected back to the crystal, which will then guide it towards the IR detector[73]. It is used mainly to study the surface of samples[72,73].

2.2.5. Water contact angle

Contact angle is used in order to determine the hydrophobicity or hydrophilicity of a surface, by means of a drop of water placed on top of the surface of interest. It is generally accepted that a contact angle higher than 90º corresponds to a hydrophobic material, and a contact angle lower than 90º belongs to a hydrophilic one[74]. Fig. 5 depicts the degree of wettability based upon the contact angle.

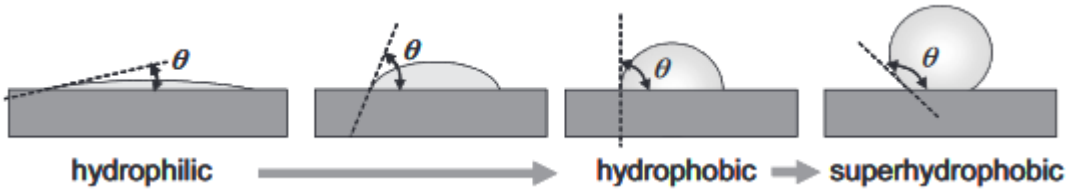

Fig. 5 Degree of wettability during water contact angle measurements. Taken from Förch R., Surface design: Applications in Bioscience and Nanotechnology, 2009.

3. Experimental part

3.1. Polymer dispersion preparation

Polyethylene oxide (PEO), approx. M.W. 600,000, was dissolved in water to obtain a 6 wt% solution (3 g of PEO in 47 g of distilled water). The PEO used in this study was obtained from Acros Organics.

Three different cellulose nanofibrils (CNF)/water solutions were used in this thesis, 0.691%, 0.461% and 0.346% weight/volume. The CNF solutions were prepared from the 0.691% CNF solution by diluting it with distilled water. 0.461% CNF dilution was prepared by mixing two parts of 0.691% CNF solution with one part of distilled water. 0.346% CNF was prepared by mixing one part of 0.691% CNF solution with one part of distilled water. The CNF used in this thesis work was provided by the Laboratory of Wood and Paper Chemistry at Åbo Akademi University and stored in fridge.

A commercial solution of poly(3,4-ethylenedioxythiophene) doped with polystyrene sulfonate (PEDOT:PSS) was also used in the preparation of the polymer dispersion. Concentration of this solution was 1.3% PEDOT:PSS in water (0.5wt-% PEDOT, 0.8wt-% PSS), with an electrical conductivity of 1 S/cm. This PEDOT:PSS dispersion was obtained from Sigma-Aldrich and stored in fridge.

2 different polymer dispersions were used in this work. The first dispersion was made of 2 g of CNF of the desired concentration, 8 g of 6wt% PEO and 4 ml of PEDOT:PSS (0.143 g/ml CNF, 0.571 g/ml PEO 6% and 0.286 ml/ml PEDOT:PSS 1.3%). The second dispersion's composition consisted of 2 g of CNF of the desired concentration, 7 g of 6wt% PEO and 5 ml of PEDOT:PSS (0.143 g/ml CNF, 0.5 g/ml PEO 6% and 0.357 ml/ml PEDOT:PSS 1.3%). Both dispersions had an approximate volume of 14 ml.

Preparation of the polymer dispersions was performed as follows:

CNF of the desired concentration was weighed in a glass vial, afterwards PEO was weighed in the same vial. This mixture was then magnetically stirred for 5 h. After stirring, PEDOT:PSS was poured into the mixture with an automatic pipette and stirred for 6 h. When the stirring process was finished, the resulting dispersion was stored in fridge until it was needed for electrospinning.

Before the electrospinning was performed, the dispersion was taken out of the fridge and allowed to reach room temperature for an hour before the addition of the desired volume of poly(ethylene glycol) diglycidyl ether (PEGDE). PEGDE was added to the polymer dispersion to function as a crosslinker, providing a degree of water resistivity

to the nanofibers obtained from the electrospinning process. PEGDE used in this work was obtained from Sigma-Aldrich and used as such. It was also stored in fridge.

Besides the previously mentioned polymer dispersions, three additional dispersions without CNF were prepared. The preparation procedure for these dispersions was the same as that used for the dispersions with CNF. The first dispersion contained 7 g of 6wt% PEO and 5 ml of PEDOT:PSS (0.583 g/ml PEO 6% and 0.417 ml/ml PEDOT:PSS 1.3%), the second dispersion contained 8 g of 6wt% PEO and 4 ml of PEDOT:PSS (0.666 g/ml PEO 6% and 0.334 ml/ml PEDOT:PSS 1.3%) and the third dispersion was made up of 9 g of 6wt% PEO and 5 ml PEDOT:PSS (0.643 g/ml PEO 6% and 0.357 ml/ml PEDOT:PSS 1.3%).

3.2. Electrospinning

The electrospinning process was performed as follows:

2 ml of the polymer dispersion was pipetted into a 10 ml glass beaker, and enough volume of PEGDE was added to it in order to reach a concentration of 0.714 µl PEGDE/ml (0.01 ml of PEGDE per 14 ml of polymer dispersion) and magnetically stirred for 20 min before starting the electrospinning process.

This dispersion was then transferred with the help of an automatic pipette to a 5 ml plastic syringe, fitted with a blunt tip metallic needle. The syringe was placed on the electrospinning setup and prepared for the electrospinning process.

The electrospinning setup consisted of a pumping machine KDS Legato 200 series from KDScientific, which was responsible of controlling the pumping rate at which the polymer dispersion was propelled out of the syringe. A metallic collector plate, covered with aluminum foil, was placed 15 cm from the blunt tip of the needle. A power source PS/ER75P04.0GM1 from Glassman High Voltage Inc., was connected to the setup via 2 caiman clips. One caiman clip was attached to the needle and the other was attached to the collector plate, in order to ground it.

Two different electrospinning parameters were utilized in this thesis, which are described in Table 1.

Fibers obtained from this process were collected on a piece of aluminum foil, in order to perform SEM measurements to observe the morphology of the fibers and to observe water contact angles, and over indium tin oxide (ITO) glass, to perform cyclic voltammetric measurements.

The ITO glasses used to collect the fibers were cleaned before each electrospinning experiment, according to the following procedure. The glasses were placed in chloroform and subjected to an ultrasonic bath for 10 min. After this ultrasonic bath, the ITO glasses were taken out of the chloroform and placed in acetone, and then placed in the ultrasonic bath for 10 min. Following sonication in acetone, the ITO glasses were taken out of the solution and left to dry in air before being weighed.

Table 1 Electrospinning conditions

	Parameter set 1	Parameter set 2
Applied voltage, kV	20	25
Pumping rate, ml/h	0.5	0.6
Spinning time, h	1	1
Collector plate distance from needle tip, cm	15	15

The surface area of the ITO glasses subjected to the electrospinning process was kept as 1 cm^2. In order to have 1 cm^2 of ITO glass, the surface of the glass was covered with aluminum foil, and 14.3 mm of the glass (width 7 mm) was left uncovered for the fibers to be deposited over it.

3.3. Scanning Electron Microscopy

SEM was performed in order to observe the morphology of the fibers. Dispersions used for the SEM measurements are described in Table 2.

The SEM instrument used in this thesis was a LEO Gemini 1520 with a Thermo Scientific Ultra Dry Silicon Drift Detector (SDD). Detector used for the images presented in this work was the In-lens detector of the instrument. Sputter coater was an Emscope TB 500 Temcarb, which coated the samples with a layer of carbon through evaporation.

The fiber dimensions were measured with the help of the free software ImageJ, version 1.52n

Table 2 Polymer compositions used for SEM studies

Sample ID	**CNF, %**	**PEGDE, ml per 14 ml**	**Potential applied, kV**	**Pumping rate, ml/h**	**PEDOT:PSS, ml per 14 ml**	**6wt% PEO, g**
1A1	0.691	0.01	20	0.5	4	8
2A1	0.691	0.01	20	0.4	4	8
3A1	0.691	0.01	20	0.6	4	8
4A1	0.691	0.01	25	0.6	4	8
5A1	0.691	0.01	25	0.4	4	8
6A1	0.691	0.01	25	0.5	4	8
1A2	0.461	0.1	20	0.5	4	8
2A2	0.461	0.01	20	0.5	4	8
3A2	0.461	0.01	20	0.4	4	8
4A2	0.461	0.01	20	0.6	4	8
5A2	0.461	0.01	25	0.6	4	8
6A2	0.461	0.01	25	0.4	4	8
7A2	0.461	0.05	25	0.5	4	8

Sample ID	CNF, %	PEGDE, ml per 14 ml	Potential applied, kV	Pumping rate, ml/h	PEDOT:PSS, ml per 14 ml	6wt% PEO, g
8A2	0.461	0.05	20	0.5	4	8
1A3	0.346	0.01	20	0.5	4	8
2A3	0.346	0.01	20	0.4	4	8
3A3	0.346	0.01	20	0.6	4	8
4A3	0.346	0.01	25	0.6	4	8
5A3	0.346	0.01	25	0.4	4	8
6A3	0.346	0.01	25	0.5	4	8
A1	0	0	20	0.5	4	8
A2	0	0	20	0.5	5	7
A3	0	0.01	20	0.5	4	8
A4	0	0.01	20	0.5	5	7
A5	0.691	0	20	0.5	4	8
A6	0.691	0	20	0.5	5	7
A7	0.691	0	25	0.6	4	8
A8	0.691	0	25	0.6	5	7
A9	0.691	0.1	20	0.5	4	8
A10	0.691	0.1	20	0.5	5	7
A11	0.691	0.1	25	0.6	4	8
A12	0.691	0.1	25	0.6	5	7
A13	0.691	0.05	25	0.6	5	7
A14	0.691	0.01	20	0.5	5	7
A15	0.691	0.01	25	0.6	5	7
A16	0.691	0.005	25	0.6	5	7
A17	0	0.01	20	0.5	5	9
A18	0.461	0	20	0.5	5	7
A19	0.461	0	20	0.5	4	8
A20	0.461	0.01	20	0.5	5	7
A21	0.461	0.005	20	0.5	4	8
A22	0.461	0.001	20	0.5	4	8
A23	0.346	0	20	0.5	5	7
A24	0.346	0	20	0.5	4	8
A25	0.346	0.01	20	0.5	5	7
A26	0.346	0.01	25	0.6	5	7
A27	0.691	0.01	25	0.6	5	7

3.4. Cyclic Voltammetry

In order to measure the electrochemical properties of the electrospun fibers, cyclic voltammetric (CV) measurements were performed.

All CV experiments were performed in a 0.1 M KCl solution, which was deaerated with a stream of N_2 gas for 15 min prior to the measurements. The working electrode was an ITO glass, with surface of 1 cm^2 covered with electrospun nanofibers. The counter electrode was a glassy carbon (GC) rod and reference electrode consisted of a double junction Ag/AgCl (3 M KCl) electrode. Scanning potential ranged from -0.5 V to 0.5 V with a scan rate of 20 mV/s. 5 potential cycles were measured for each polymer composition, and the data from the last cycle was used in order to show the results.

The software used for the analysis of CV's was Nova 2.1.3 connected to an Autolab PGSTAT 30 potentiostat.

CV measurements were performed as follows:

21 ml of 0.1 M KCl solution was pipetted to a cylindrical glass container. The solution was then placed under a stream of N_2 for 15 min, in order to deaerated it. N_2 gas was streamed into the solution with the help of a needle attached to the end of the gas line. After this process, the ITO glass was placed in the solution and the measurement started.

Electrospun fibers using 5 different polymer dispersion compositions with 20 and 25 kV applied potential and 0.5 and 0.6 ml/h pumping rate were studied for a period of two months, in order to determine fiber behavior when subjected to long term exposure to water. Polymer compositions that were studied under these conditions are detailed in Table 3. Measurements were performed every 12 h during the first week, and once a week afterwards until two months. Electrodes were kept in 0.1 M KCl solution during the test and were only taken out of solution in order to place them in the electrochemical cell for the CV measurements.

Table 3 Polymer compositions and electrospinning parameters used for long term stability studies in water

CNF, %	PEGDE, ml per 14 ml	Potential applied, kV	Pumping rate, ml/h	PEDOT:PSS, ml per 14 ml	6wt% PEO, g
0.691	0.01	20	0.5	5	7
0.691	0.01	25	0.6	5	7
0.691	0.1	25	0.6	5	7
0.461	0.01	20	0.5	5	7
0.346	0.01	20	0.5	5	7

A second set of CV experiments was performed in order to observe how exposure to water changed the electrical properties of the fibers. These experiments were carried out for 3 days. The CV response of the fibers was measured immediately after exposure to water and 1 h, 1 day, 2 days and 3 days after exposure. Before each measurement, the electrode was left to stand in air for 1 h. Table 4 details the polymer compositions and parameters that were used for these experiments.

In addition, the mass of the ITO glasses was weighed before the electrospinning process and after the CV measurements were concluded, in order to know the mass

of fibers spun over the ITO glasses and the amount of fiber that was dissolved during the CV measurements.

Table 4 Polymer compositions and electrospinning parameters used for water exposure studies

CNF, %	PEGDE, ml per 14 ml	Potential applied, kV	Pumping rate, ml/h	PEDOT:PSS, ml per 14 ml	6wt% PEO, g
0	0.01	20	0.5	5	9
0	0.1	20	0.5	5	7
0.691	0.05	25	0.6	5	7
0.691	0.01	25	0.6	4	7
0.691	0.005	25	0.6	5	7
0.346	0.01	25	0.6	5	7

3.5. Water contact angle

Water contact angle experiments were performed in order to observe the hydrophilicity or hydrophobicity of the fibers.

10 µl of distilled water was placed with an automatic pipette on top of electrospun fibers over aluminum foil, and photographs of the drop were taken every 5^{th} s for 30 s with a digital camera.

Table 5 shows a summary of the different polymer dispersion compositions that were utilized for these measurements.

Table 5 Polymer compositions used for water contact angle observations

CNF content, %	PEGDE, ml per 14 ml	PEDOT:PSS, ml per 14 ml	Potential Applied, kV	Pumping rate, ml/h	6wt% PEO, g
0.691	-	4	20	0.5	8
0.691	-	5	20	0.5	7
0.691	-	4	25	0.6	8
0.691	-	5	25	0.6	7
0.691	0.01	5	20	0.5	7
0.691	0.01	5	25	0.6	7
0.461	-	4	20	0.5	8
0.461	0.05	4	20	0.5	8
0.461	0.005	4	20	0.5	8
0.461	0.001	4	20	0.5	8

3.6. Fourier-transform Infrared spectroscopy

Fourier transform infrared spectroscopy (FTIR) was performed on the fibers in order to determine if there was a visible change in the infrared spectra of the fibers before and after the crosslinking process with PEGDE and to understand the changes occurring in the fiber structures during water contact.

The spectra were recorded using a Harrick's VideoMVP single reflection diamond ATR accessory (incidence angle 45°) with a horizontal sampling area of Ø = 500 µm and a build-in pressure applicator. Small pieces of fibers spun on Al foil were tightly pressed against the diamond crystal and 32 interferograms were recorded with a resolution of 4 cm^{-1}. The ATR accessory was attached to a Bruker IFS 66S spectrometer equipped with a DTGS detector.

4. Results and discussion

4.1. Scanning Electron Microscopy

It was observed in the SEM images obtained in this thesis work that electrospinning conditions have a high influence over the morphology of the spun fibers. For this reason, several experiments were run in order to find the best polymer dispersion compositions and electrospinning conditions for use in this work.

The parameters used to define a uniform morphology were based upon the presence of bead-like structures and fiber appearance observed with SEM and the charging capabilities of the polymers measured with CV. Parameters related to the electrospinning process that were tested in order to observe the variations over the fibers morphology were pumping rate, 0.4, 0.5 and 0.6 ml/h and applied potential, 20 and 25 kV. Parameters related to the polymer dispersion that were tested were CNF content (0%, 0.346%, 0.461% and 0.691%), PEDGE amount (0.1, 0.05, 0.01 and 0.005 per 14 ml of polymer dispersion), PEDOT:PSS volume (4 and 5 ml per 14 ml of polymer dispersion) and 6wt% PEO content (7, 8 and 9 g per 14 ml of polymer dispersion).

Different polymer compositions electrospun under different conditions were subjected to SEM, in order to observe how fiber morphology was affected by variations in CNF content, pumping rate, applied potential, PEGDE content, 6wt% PEO content, PEDOT:PSS content and after exposure to water.

Fiber morphology was heavily reliant on applied potential and pumping rate, a behavior that was shown evident with the help of the SEM images obtained from this work and from the works of Bhardwaj and Kundu[8], Huang et al.[38] and Demir et al.[41].

4.1.1. Effect of CNF content on fiber morphology

In order to observe how the content of CNF would affect the fiber morphology, 2 ml of four different polymer dispersion compositions (0%, 0.346%, 0.461% and 0.691%) were prepared and tested under the same electrospinning parameters. The electrospinning parameters tested were pumping rate of 0.5 ml/h and an applied potential of 20 kV for the first set and pumping rate of 0.6 ml/h and an applied potential of 25 kV for the second set.

Without CNF added to the polymer dispersion, fiber morphology looked akin to modeling clay that was chopped hastily, as seen in Fig. 6a. In contrast, fibers that had CNF in their composition exhibit a morphology that more clearly resembles those of strings. Overall, the main differences in fiber morphology revolves around the presence of bead-like structures and the length of the fibers. The likelihood of these

bead-like structures appearing in the morphology of the fibers appears to be related to the CNF concentration of the polymer dispersion, as shown in Fig. 6. This likelihood increases with an increasing concentration of CNF in the polymer dispersion, when spinning with an applied potential of 20 kV and a pumping rate of 0.5 ml/h and a PEGDE volume of 0.01 ml per 14 ml of polymer dispersion, which could be due to an increase in the viscosity of the solution, as described by Fortunato et al.[56].

The nanofibers resulting from an electrospinning process with a pumping rate of 0.6 ml/h and an applied potential of 25 kV are shown in Fig. 7. The presence of bead-like structures is numerous in polymer dispersions with CNF concentrations lower than 0.5% (Figs. 7a, 7b). However, the polymer dispersion containing 0.691% CNF (Fig. 7c) exhibits fewer bead-like structures than the nanofibers spun with the same dispersion composition but spun with 0.5 ml/h pumping rate and 20 kV applied potential (Fig. 6d). At the same time, it can be observed in Fig. 7 that the number of nanofibers increases when the concentration of CNF in the polymer dispersion increases.

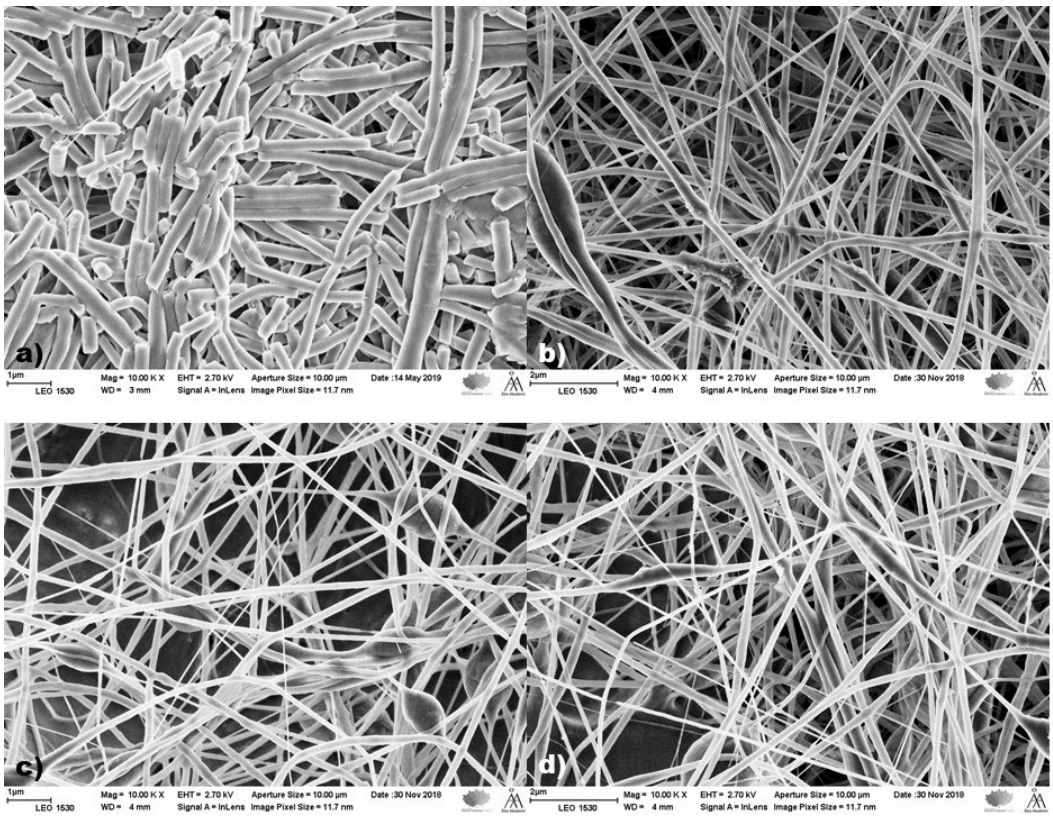

Fig. 6 SEM images of fibers made with different CNF concentrations, 0.01 ml PEGDE and 4 ml PEDOT:PSS per 14 ml of polymer dispersion, pumping rate 0.5 ml/h, applied potential 20 kV. a) No CNF b) 0.346% CNF c) 0.461% CNF d) 0.691% CNF.

One can then conclude that the CNF content will benefit fiber morphology based on the electrospinning conditions. When spinning with a pumping rate of 0.6 ml/h and an applied potential of 25 kV, fiber morphology benefits from a higher amount of CNF present in the polymer composition, while a pumping rate of 0.5 ml/h and an applied potential of 20 kV benefits fiber morphology more when CNF amount present in the polymer dispersion is lower than 0.4%.

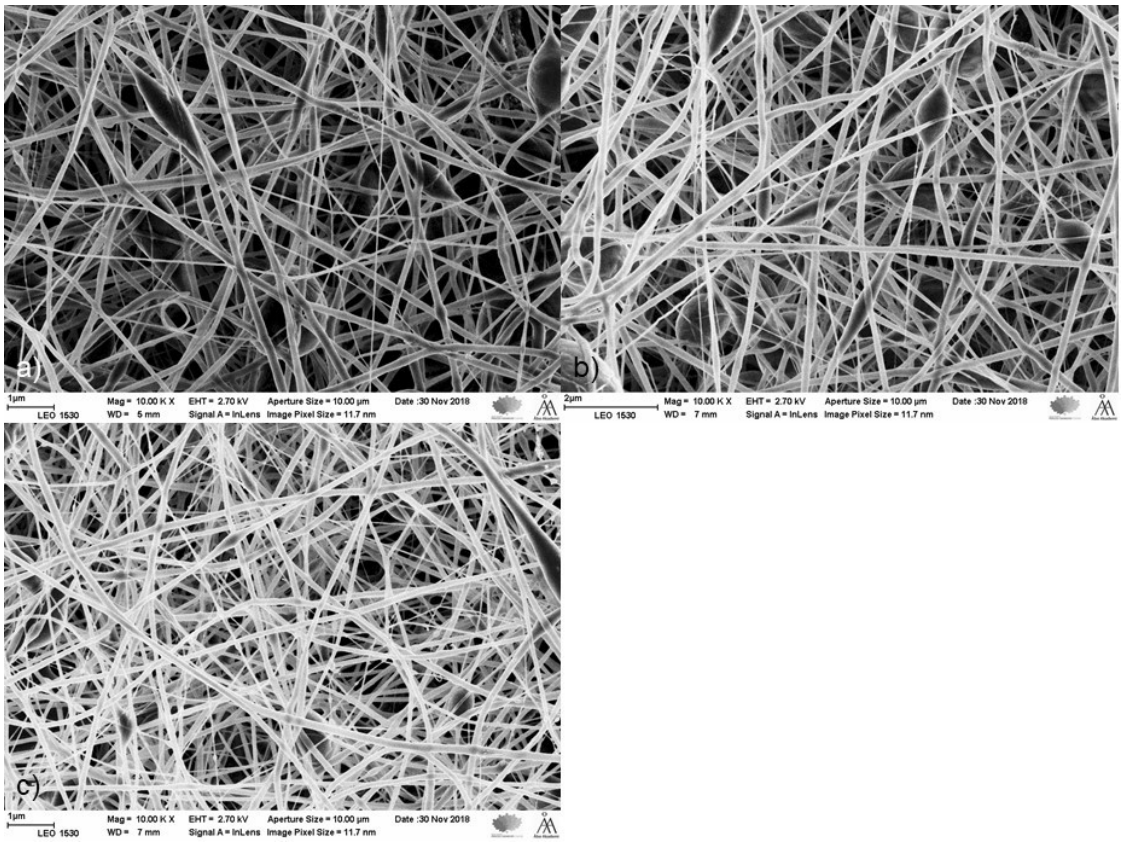

Fig. 7 SEM images of fibers made with different CNF concentrations, 0.01 ml PEGDE and 4 ml PEDOT:PSS per 14 ml of polymer dispersion, pumping rate 0.6 ml/h, applied potential 25 kV. a) 0.346% CNF b) 0.461% CNF c) 0.691% CNF.

4.1.2. Effect of pumping rate on fiber morphology

The effect of pumping rate on fiber morphology is most noticeable around the presence of the previously mentioned bead-like structures. These structures appear to be more common across morphologies of fibers with high CNF content in the dispersion that were spun with a faster pumping rate and lower applied voltage.

The presence of these bead-like structures on fibers made with polymer compositions with CNF could be related to the concentration of CNF in the polymer dispersion. The fact that the structures can be seen more frequently on morphologies that were spun at a faster pumping rate (Fig. 8, right column) suggests that the pumping speed was too high and that the polymer dispersion across the needle tip wasn't uniformly charged before being ejected from the Taylor cone towards the collector plate.

Overall, it is noticeable that the best morphology when the electrospinning process was conducted with an applied potential of 20 kV corresponds to the polymer dispersions that were electrospun with a pumping rate of 0.5 ml/h (Fig. 8, middle column).

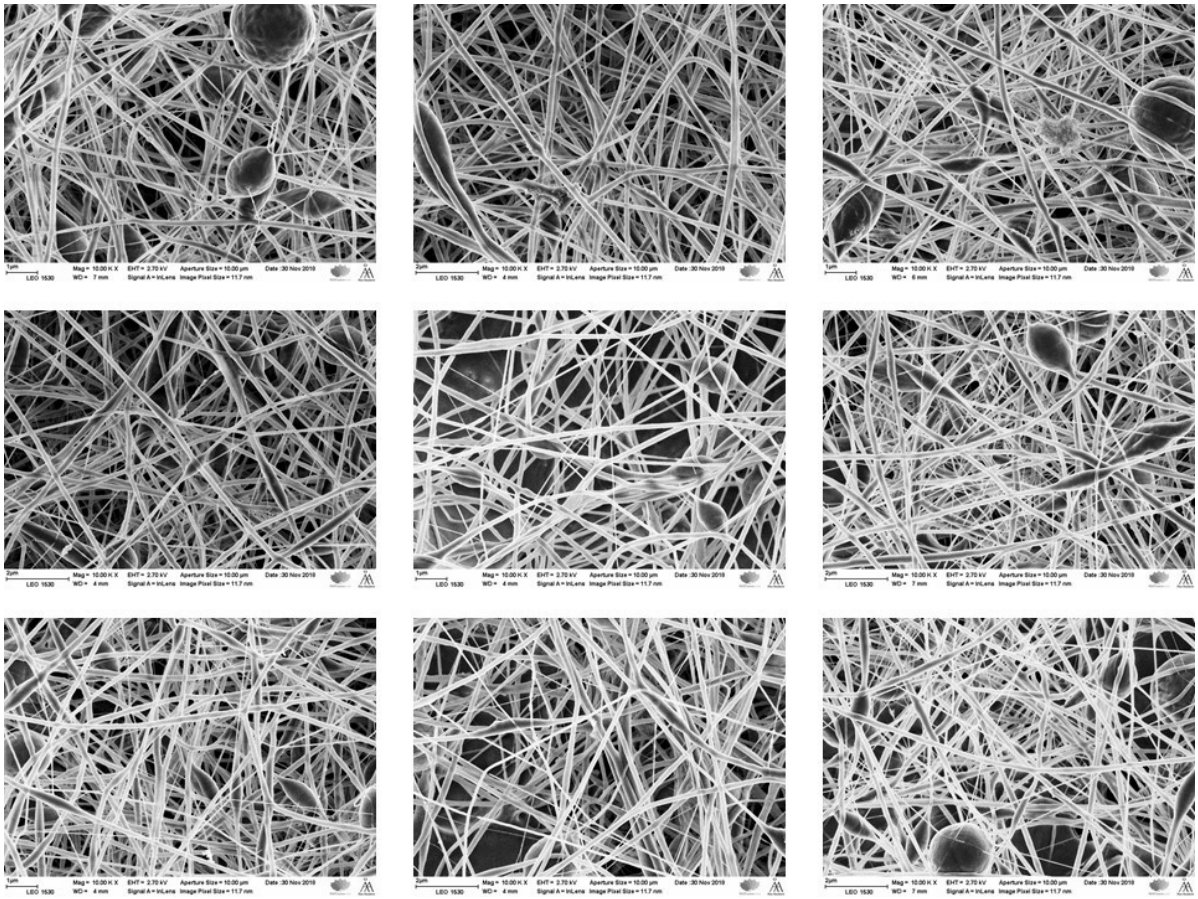

Fig. 8 SEM images of fibers made with 0.01 PEGDE and 4 ml PEDOT:PSS per 14 ml of polymer dispersion, applied potential 20 kV. Pumping rate from left to right: 0.4 ml/h, 0.5 ml/h and 0.6 ml/h. CNF content, from top to bottom: 0.346%, 0.461% and 0.691%

4.1.3. Effect of applied potential on fiber morphology

According to Bhardwaj & Kundu[8], one of the parameters that heavily impacts fiber morphology is the potential applied during the electrospinning process.

It was observed that the effect of increasing the potential applied on the polymer dispersions used in this work was related to the concentration of CNF in the dispersions. The most noticeable parameter, and the one that was used to determine whether the morphology improved, was the decrease in the presence of bead-like structures in the morphology.

Electrospinning at a higher potential had an interesting effect on fiber morphology. Fig. 8 showcases the fibers resulting from an electrospinning process with 20 kV of applied voltage. When comparing those morphologies to the ones shown in Fig. 9, it can be seen that the presence of bead-like structures on the fastest pumping rate (right column) diminished with the increase of applied potential, suggesting that an increase in applied potential coupled with an increase in pumping rate is beneficial for polymer compositions with high CNF content. The increase on applied potential, however, had an adverse effect on the composition with 0.461% CNF, giving the fibers a more “glued” appearance than when the pumping rate was 0.5 ml/h.

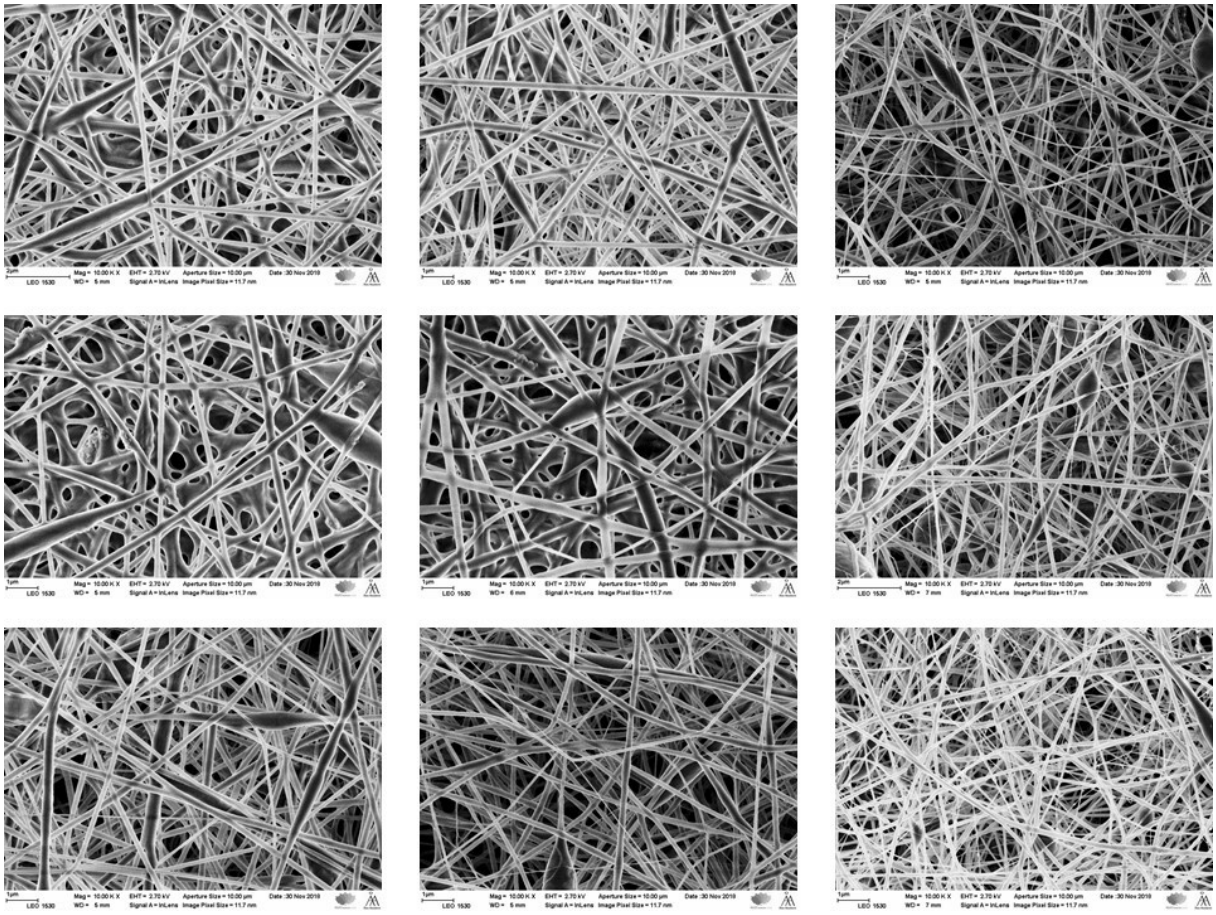

Fig. 9 SEM images of fibers made with 0.01 PEGDE and 4 ml PEDOT:PSS per 14 ml of polymer dispersion, applied potential 25 kV. Pumping rate, from left to right: 0.4 ml/h, 0.5 ml/h and 0.6 ml/h. CNF content from top to bottom: 0.346%, 0.461% and 0.691%

The effect of the applied potential can be better observed in fig. 10. When electrospinning with a pumping rate of 0.5 ml/h, the presence of bead-like structures on both 20 and 25 kV is minimal, however, there is a decrease in the amount of fibers present in the setup with a higher applied potential. However, when the pumping rate was increased to 0.6 ml/h, the morphology of the fibers changed completely. The amount of fibers visible is higher when the potential was increased to 25 kV compared to 20 kV of applied potential and the presence of bead-like structures is almost null when comparing to the same pumping rate but with 20 kV of applied potential.

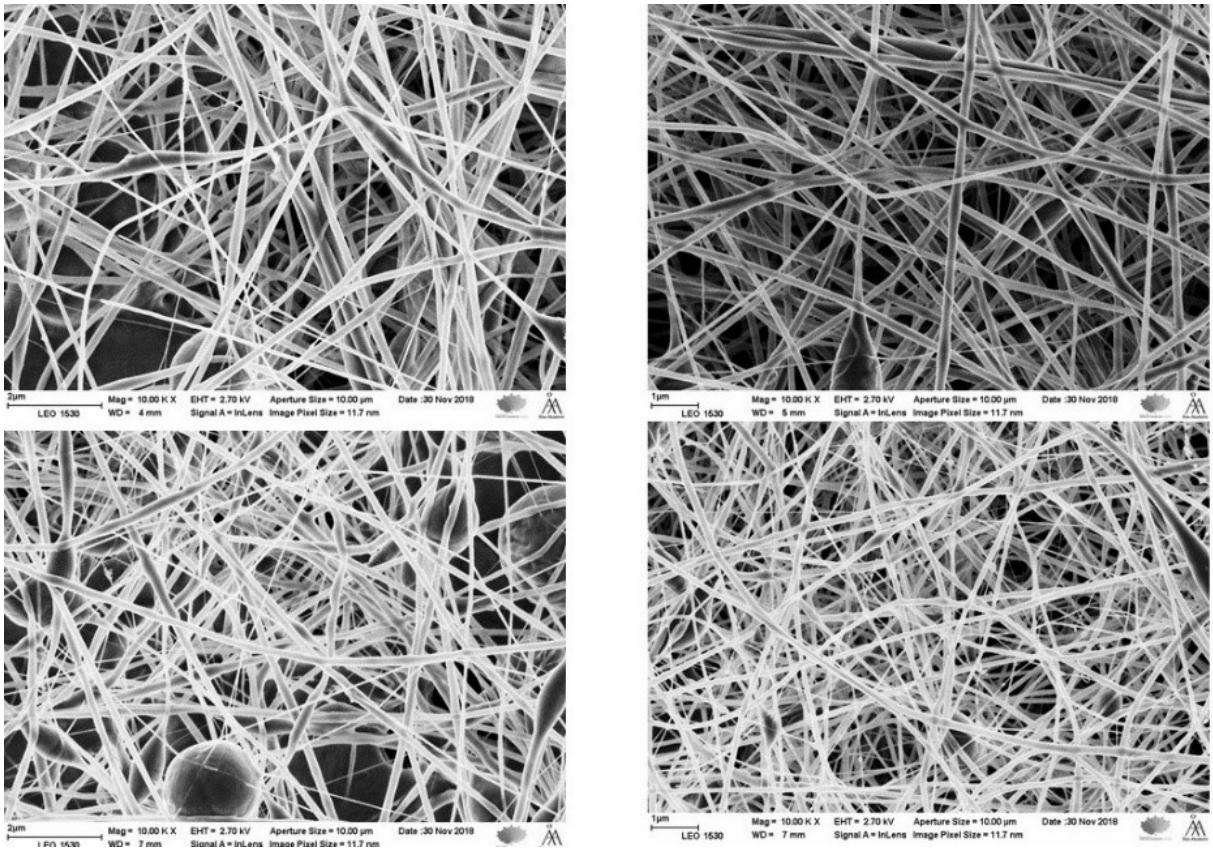

Fig. 10 SEM images of fibers made with 0.691% CNF, 0.01 PEGDE and 4 ml PEDOT:PSS per 14 ml of polymer dispersion. Pumping rate, from top to bottom: 0.5 ml/h and 0.6 ml/h. Applied potential, from left to right: 20 kV and 25 kV.

4.1.4. Effect of PEGDE content on fiber morphology

PEDGE was added to the polymer dispersion to act as a crosslinker for the components in the dispersion and to impart water resistivity to the fibers.

It can be seen in Figs. 11 and 12 that the addition of PEGDE to the polymer dispersion helps to define the structure of the nanofibers. Increasing amounts of PEGDE creates a more defined web of threads, until a certain point. Higher amounts of PEGDE (0.1 ml per 14 ml of polymer dispersion) had an adverse effect on morphology, as shown in Figs.11f) and 12e), resulting in severed threads and broader bead-like structures than dispersions with lower PEGDE volumes, such as Figs. 11e) and 12c). PEGDE had no effect over the presence and morphology of the bead-like structures.

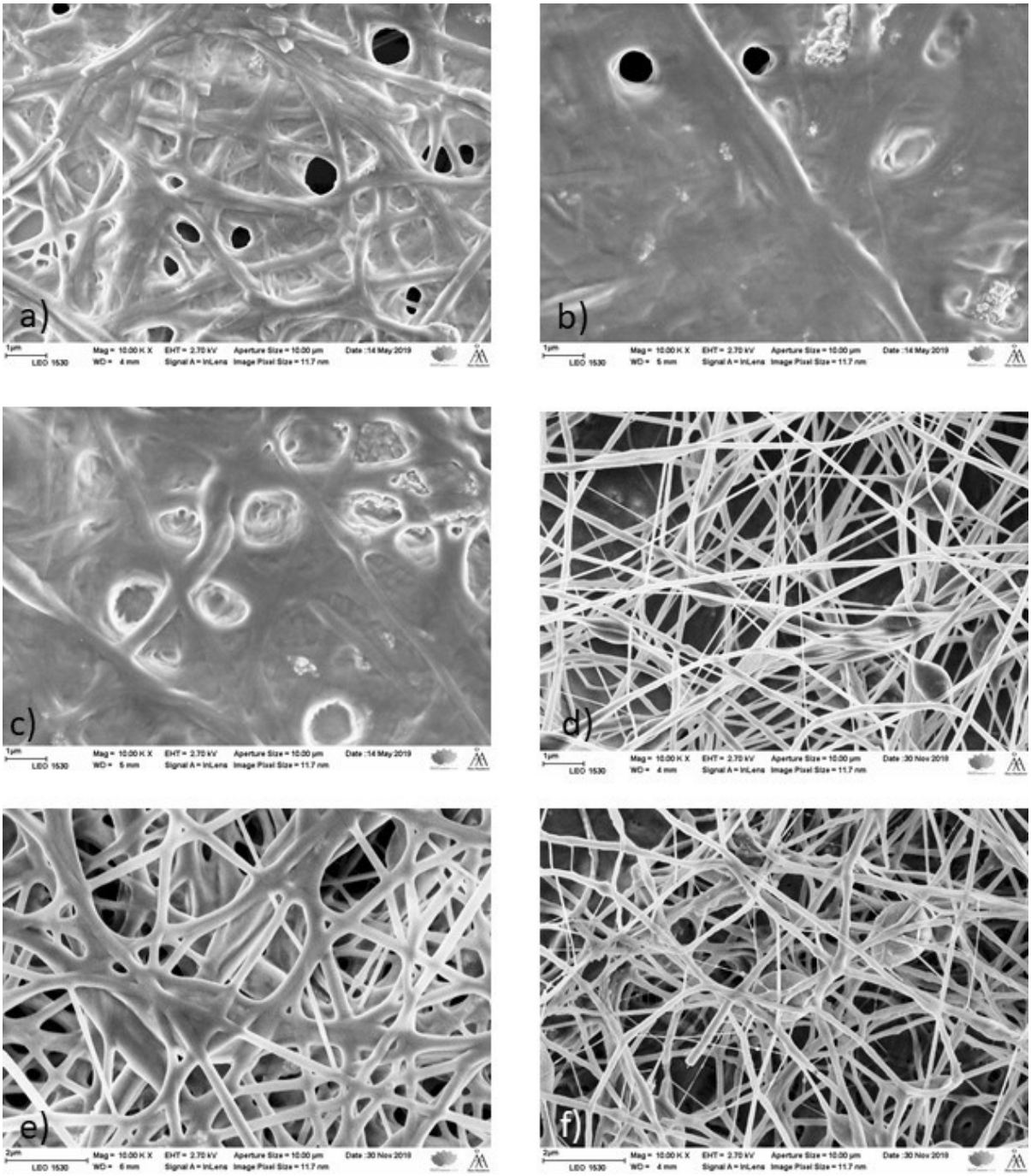

Fig. 11 SEM images of fibers made with 0.461% CNF and 4 ml PEDOT:PSS per 14 ml of polymer dispersion. Pumping rate 0.5 ml/h, applied potential 20 kV. PEGDE amount (ml per 14 ml of polymer dispersion): a) 0 ml b) 0.001 ml c) 0.005 ml d) 0.01 ml e) 0.05 ml f) 0.1 ml

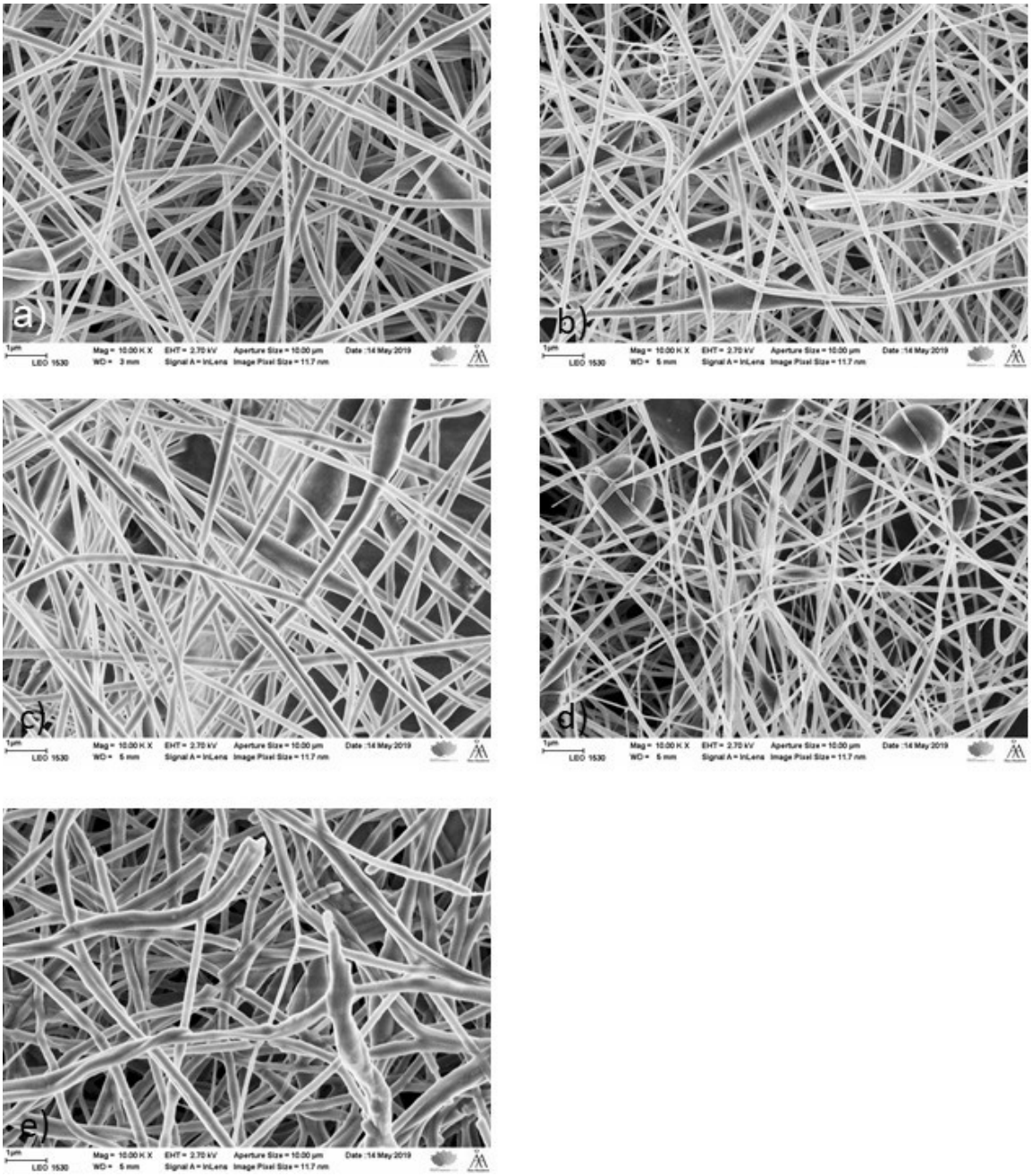

Fig. 12 SEM images of fibers made with 0.691% CNF and 5 ml PEDOT:PSS per 14 ml of polymer dispersion. Pumping rate 0.6 ml/h, applied potential 25 kV. PEGDE volume (ml per 14 ml of polymer dispersion): a) 0 ml b) 0.005 ml c) 0.01 ml d) 0.05 ml e) 0.1 ml

From these images, it was decided that the optimum content of PEGDE to obtain the best morphology when electrospinning with an applied potential of 20 or 25 kV was 0.01 ml per 14 ml of polymer dispersion.

4.1.5. Effect of PEO content on fiber morphology

Fig. 13 shows how PEO content affects the morphology of the fibers. The higher the concentration PEO in the dispersion (0.583 g/ml, left, vs. 0.642 g/ml, right) the more defined the fibers become.

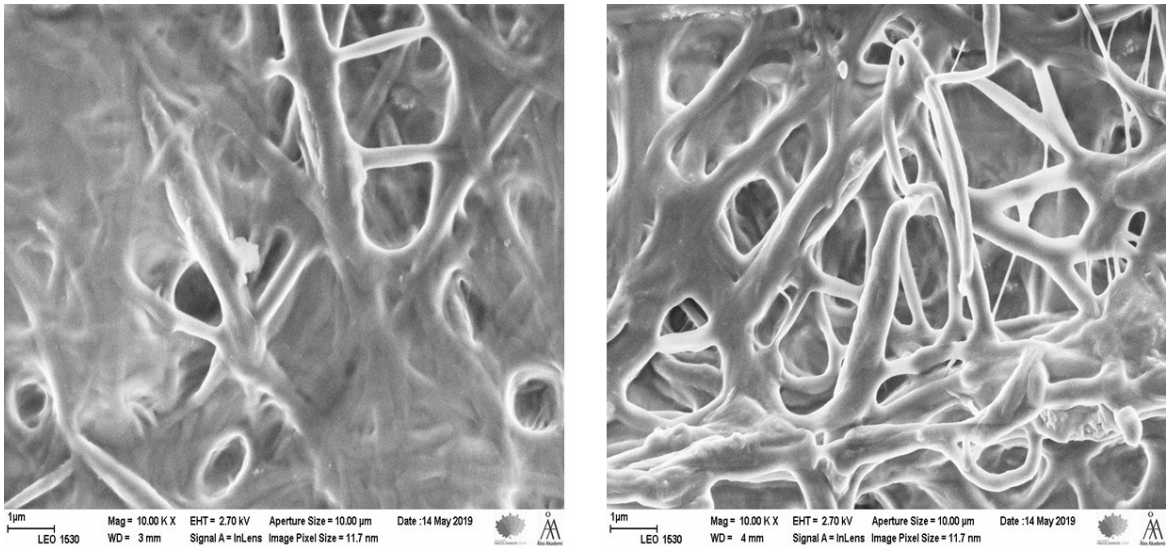

Fig. 13 SEM images of fibers made with different 6wt% PEO masses. Left: 7g 6wt% PEO Right: 9 g 6wt% PEO. Pumping rate 0.5 ml/h, applied potential 20 kV, 0.01 ml PEGDE and 5 ml PEDOT:PSS per 14 ml of polymer dispersion, no CNF.

4.1.6. Effect of PEDOT:PSS content on fiber morphology

One of the objectives of this thesis was to obtain of fibers that possess electrical activity. For this reason, the effects of the content of the conducting polymer PEDOT:PSS over the fiber morphology were studied.

Two different PEDOT:PSS concentrations were studied in this work, 4 ml PEDOT:PSS (0.286 ml PEDOT:PSS/ml) and 5 ml PEDOT:PSS (0.357 ml PEDOT:PSS/ml).

Across all polymer dispersion, when electrospinning with a pumping rate of 0.5 ml/h and an applied potential of 20 kV, the morphology of the fibers was better with 4 ml than with 5 ml PEDOT:PSS the closer to 0 the CNF content was, as can be seen in Fig. 14. However, when the CNF concentration was raised above 0.346%, the morphology of the fibers improved with more PEDOT:PSS in the dispersion. When 0.461% CNF and 5 ml PEDOT:PSS/14 ml was used (Fig. 14f), the fibers had the best morphology, presenting a high amount of fibers and a low amount of bead-like structures.

On the other hand, Fig. 15 shows the effects on fiber morphology when the pumping rate was increased to 0.6 ml/h and the applied potential to 25 kV. It can be seen in the SEM images that by utilizing polymer dispersions with higher content of CNF a higher amount and thinner fibers can be obtained, while dispersions with lower CNF content present a morphology that doesn't allow for an easy fiber identification.

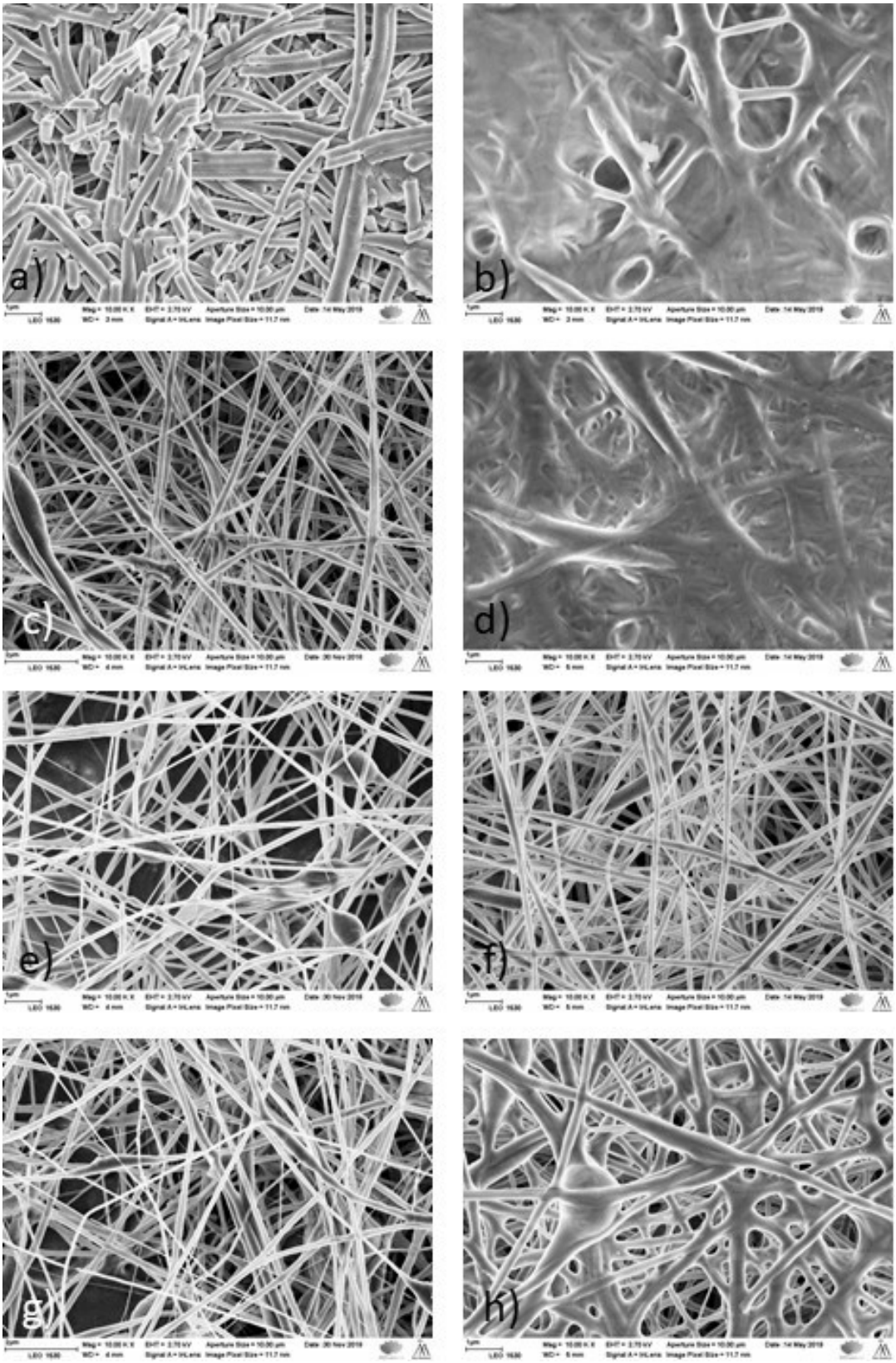

Fig. 14 SEM images of fibers showcasing the effect of PEDOT:PSS. Pumping rate 0.5 ml/h, applied potential 20 kV, 0.01 ml PEDGE per 14 ml of polymer dispersion. Left: 4 ml PEDOT:PSS per 14 ml of polymer dispersion Right: 5 ml PEDOT:PSS per 14 ml of polymer dispersion. Top to bottom: No CNF, 0.346% CNF, 0.461% CNF, 0.691% CNF.

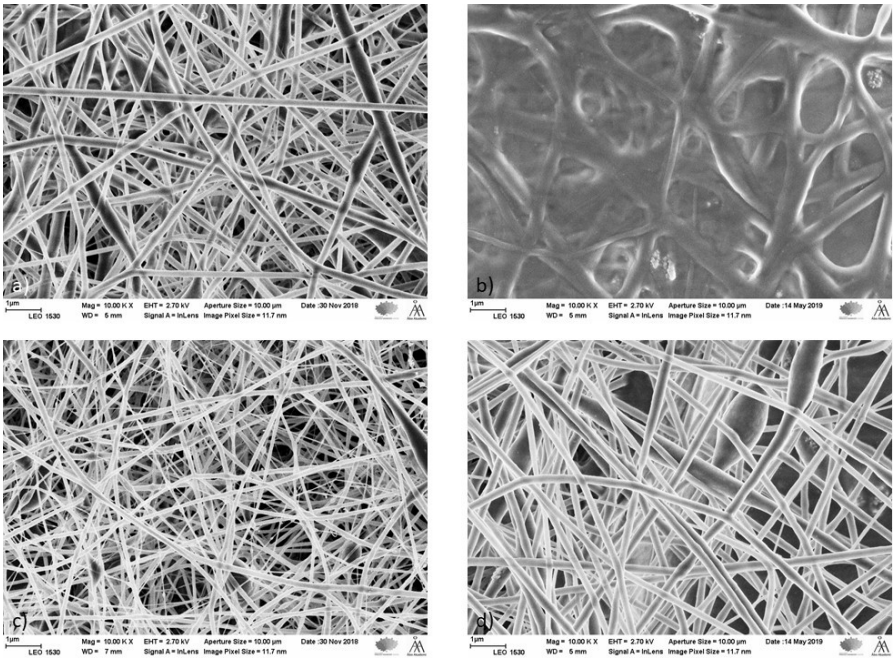

Fig. 15 SEM images of fibers showcasing the effect of PEDOT:PSS. Pumping rate 0.6 ml/h, applied potential 25 kV, 0.01 ml PEGDE per 14 ml of polymer dispersion. a) 4 ml PEDOT:PSS, 0.346% CNF b) 5 ml PEDOT:PSS, 0.346% CNF c) 4 ml PEDOT:PSS, 0.691% CNF d) 5 ml PEDOT:PSS, 0.691% CNF

4.1.7. Effect of water exposure on fiber morphology

The effect water had over the morphology of the fibers was studied by submerging a piece of aluminum foil covered with the fiber in water. This piece of aluminum was left in water for one hour, and then taken out and left to dry in air. A SEM image of the morphology of the fiber before and after water exposure can be observed in Fig. 16.

After being exposed to water, the morphology of the fibers underwent a severe change. From clearly defined threads of fibers visible in Fig. 16a, the surface morphology changed to a motif that resembles a relief, in Fig. 16b. It is still possible to see threads after water exposure; however, the fibers are broader than right after electrospinning and nearly double their diameter. It can also be appreciated that most of them appear to have mashed up in the background, forming a sort of “platform” from which some broad threads can be seen branching out of the background.

This behavior suggests that after water exposure, the cellulose present in the composition of the polymer “soaks” up water and broadens the fibers. The FTIR results (discussed later in this thesis) also suggest that some part of PEO in the fibers is dissolved during water exposure. The effect that this broadening of the fibers has over the electrical activity will be discussed in more detail in the cyclic voltammetry section of this thesis.

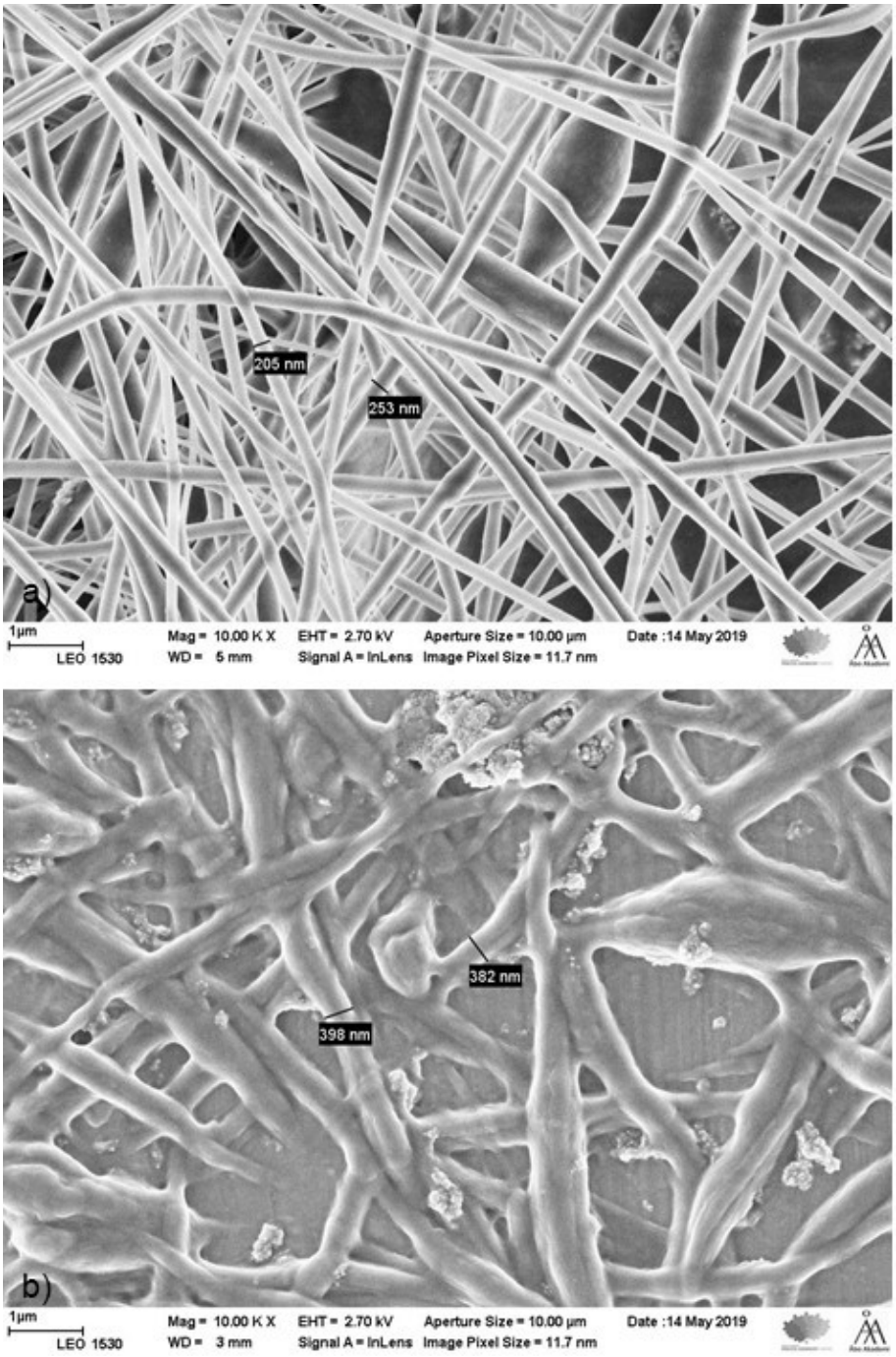

Fig. 16 SEM images of fibers made with 0.691% CNF, 0.01 PEGDE and 5 ml PEDOT:PSS per 14 ml of polymer dispersion, applied potential 25 kV, pumping rate 0.6 ml/h. a): before water exposure b): after 1-hour exposure to water.

4.2. Cyclic Voltammetry

Cyclic voltammetry (CV) measurements were performed on the electrospun nanofibers on top of ITO glass in 0.1 M KCl in order to observe the response of what different polymer compositions had on the electroactivity of the nanofibers. Overall, nanofibers electrospun from polymer dispersion compositions made with 0.691% CNF, 0.01 ml PEGDE and 5 ml PEDOT:PSS per 14 ml of polymer dispersion with an applied potential of 25 kV and a pumping rate of 0.6 ml/h and nanofibers electrospun from polymer dispersion compositions made with 0.461% CNF, 0.01 ml PEGDE and

5 ml PEDOT:PSS per 14 ml of polymer dispersion with an applied potential of 20 kV and a pumping rate of 0.5 ml/h exhibited the highest electroactivity of all the compositions tested. On the other hand, nanofibers electrospun from polymer dispersion compositions containing 4 ml PEDOT:PSS per 14 ml of polymer dispersion exhibited poor electrical capabilities, independently of CNF or PEGDE content.

The ejection of the charged polymer dispersion composition from the Taylor cone to the collector plate is a chaotic event, with little to none possibility of controlling where the electrospun nanofibers will be deposited. Having a large area to collect the nanofibers helps, but with an electrode surface of only 1 cm^2, it was not possible to ensure that all the electrodes were collecting the same mass of nanofibers upon their surface during every electrospinning experiment. For this reason, for the experiments concerning nanofiber long term stability in water and the effect or drying before measuring the CV's, the mass of the ITO glass was measured before the electrospinning process and after, in order to determine the mass of the nanofibers collected. This data was considered in the CV's by dividing the current by the nanofibers mass, to account for mass variations that could occur during the electrospinning process.

4.2.1. Effect of PEDOT:PSS content on charging capacities

The effect of PEDOT:PSS concentration over the charging capacities of the polymer was studied utilizing polymer dispersion compositions with 0.691% CNF and 0.01 ml per 14 ml PEGDE, electrospun with a pumping rate of 0.6 ml/h and an applied potential of 25 kV.

Fig. 17 showcases the differences in the charging capacities observed. As it was expected, an increase in the amount of conducting polymer present in the polymer compositions lead to an increase in the charging capability of the polymer.

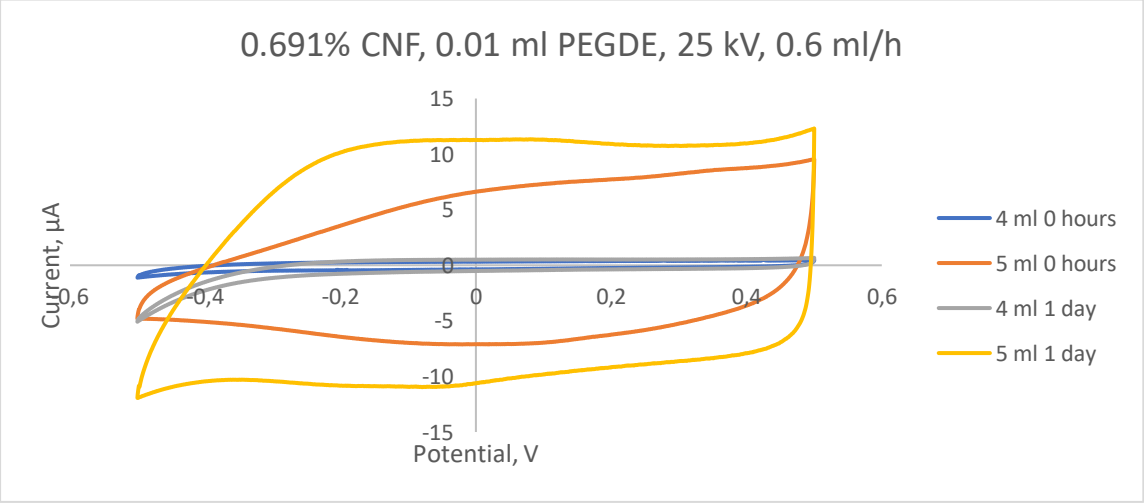

Fig. 17 CVs of electrospun fibers with different PEDOT:PSS content. Supporting electrolyte: 0.1 M KCl, potential scan rate: 20 mV/s.

4.2.2. Long-term polymer stability in 0.1 M KCl

Long term stability studies were conducted for a period of 2 months on five different polymer compositions. The polymer compositions studied are detailed in Table 6.

Table 6 Polymer dispersions used for spinning of fibers subjected to long-term stability studies

Polymer dispersion composition	CNF, %	PEGDE, ml per 14 ml	Pumping rate, ml/h	Applied potential, kV	PEDOT:PSS, ml per 14 ml	Fiber mass, mg
1	0.691	0.01	0.5	20	5	1.6
2	0.691	0.01	0.6	25	5	1.2
3	0.691	0.1	0.6	25	5	0.5
4	0.461	0.01	0.5	20	5	1.1
5	0.346	0.01	0.5	20	5	1.1

All polymer compositions studied for long term stability exhibited a capacitor like behavior, as well as good stability when been in contact with 0.1 M KCl solution.

Polymer dispersion compositions 1 and 2 depicted in Table 6 were studied in order to observe the effect that fiber morphology had over the stability and the charging capabilities of the nanofibers. It can be observed in Figs. 18 and 19 that both polymer compositions behaved similarly during the first hours after being submerged in electrolyte solution, however, the degradation rate of the fibers, linked to a decay in charging capabilities, was faster in the polymer composition electro spun at 20 kV of applied potential and 0.5 ml/h pumping rate. This decay in charging capabilities correlates to observations made with SEM, in which faster pumping rates and higher applied potentials were more beneficial to the morphology of polymer compositions with 0.691% CNF content.

Fig. 20 showcases the effect that a higher PEGDE concentration had on the charging capabilities of the polymer. It can be seen when comparing CVs shown in Figs. 18 and 19 with CVs in Fig. 20 that the charging capabilities of the polymer are almost halved with a ten-fold increase in PEGDE concentration. This could be due to morphology differences between the nanofibers, as it can be seen in Fig. 12. With 0.1 ml PEGDE per 14 ml of polymer dispersion, the fibers become shorter and broader (Fig. 12e) in comparison to 0.01 ml PEGDE per 14 ml of polymer dispersion (Fig. 12c) which showcases thinner and longer fibers. However, the capacitor like behavior is kept, and the stability of the polymers is good, aside of showing a diminished charging capability with higher PEGDE content.

When the fibers with lower PEGDE content were studied, it could be observed that the fibers were dissolving in the solution. This was detected visually, by a black-blueish substance dripping from the ITO glass surface to the bottom of the glass cell. For this reason, the lowest PEGDE content studied was 0.005 ml PEGDE per 14 ml of polymer dispersion.

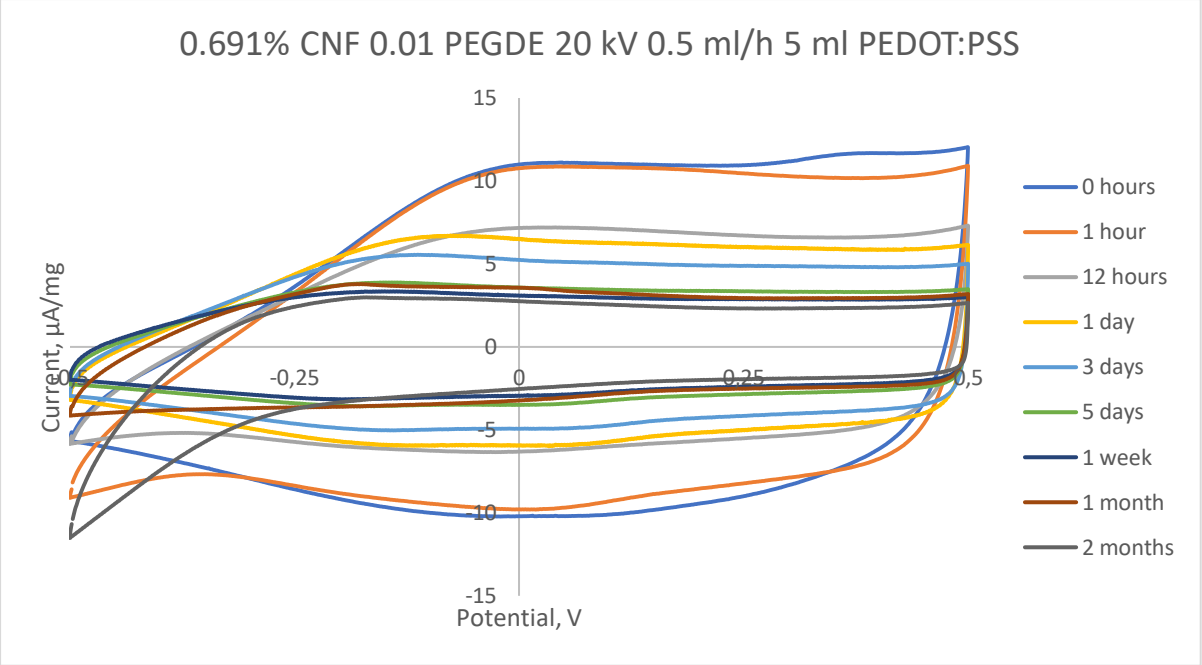

Fig. 18 Long term stability CVs of electrospun nanofibers. Supporting electrolyte 0.1 M KCl, scan rate 20 mV/s. 0.691% CNF, 0.01 ml PEGDE and 5 ml PEDOT:PSS per 14 ml of polymer dispersion, pumping rate 0.5 ml/h, applied potential 20 kV.

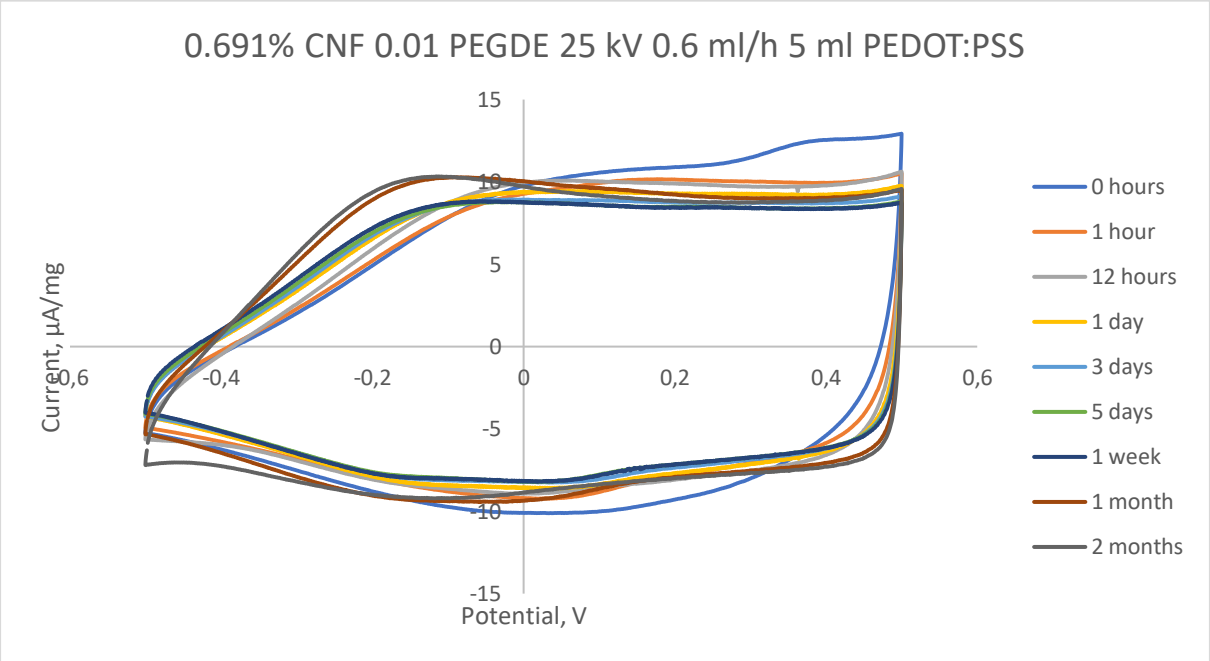

Fig. 19 Long term stability CVs of electrospun nanofibers. Supporting electrolyte 0.1 M KCl, scan rate 20 mV/s. 0.691% CNF, 0.01 ml PEGDE and 5 ml PEDOT:PSS per 14 ml of polymer dispersion, pumping rate 0.6 ml/h, applied potential 25 kV.

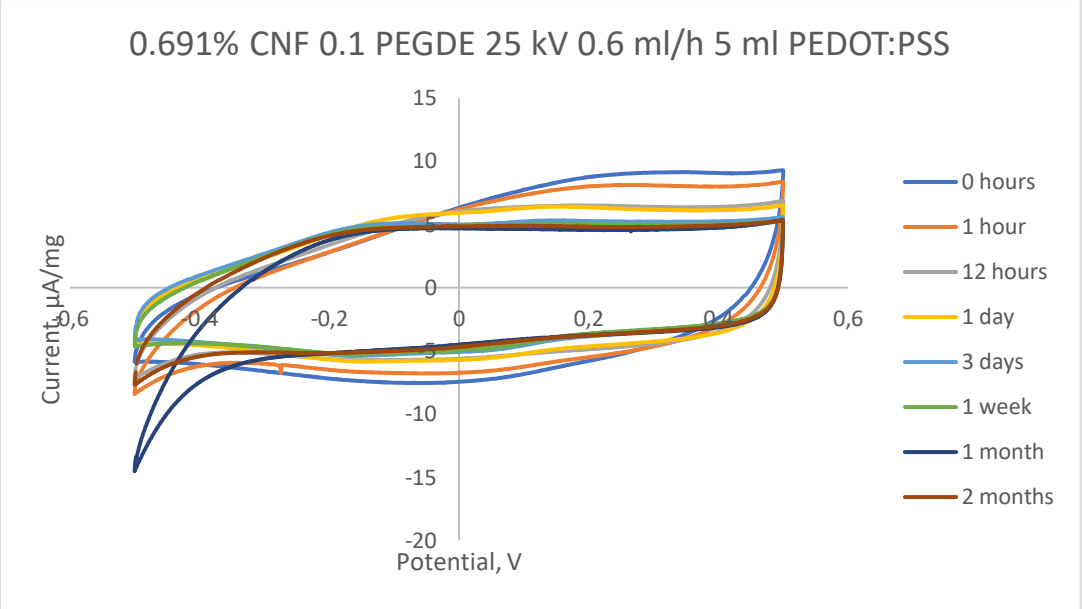

Fig. 20 Long term stability CVs of electrospun nanofibers. Supporting electrolyte 0.1 M KCl, scan rate 20 mV/s. 0.691% CNF, 0.1 ml PEGDE and 5 ml PEDOT:PSS per 14 ml of polymer dispersion, pumping rate 0.6 ml/h, applied potential 25 kV.

Besides the long-term stability studies performed with nanofibers electrospun from a polymer dispersion with 0.691% CNF and spun under the best conditions, nanofibers from two other polymer solutions with different CNF content were studied for long term stability.

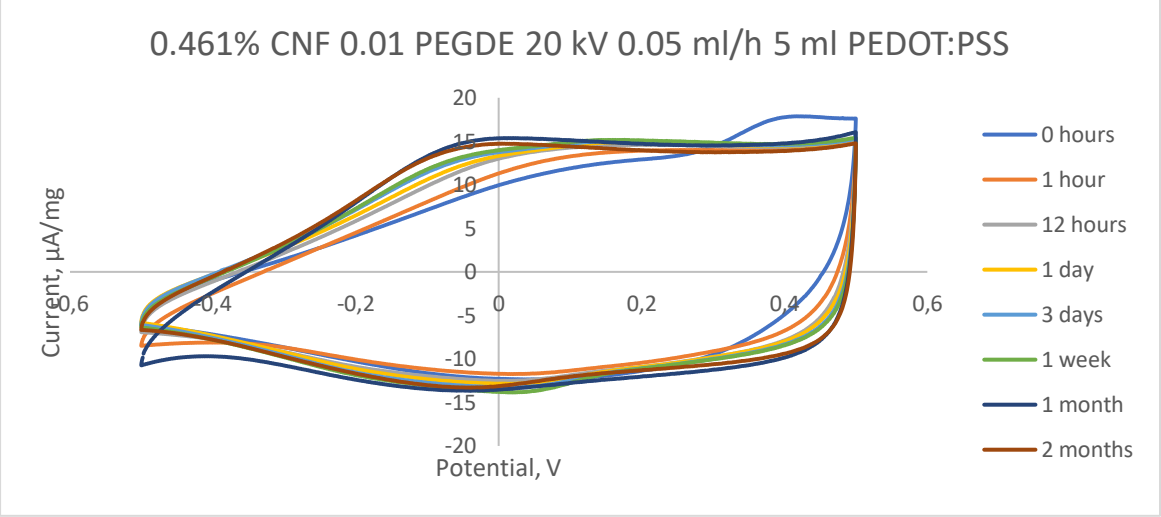

Fig. 21 Long term stability CVs of eletrospun nanofibers. Supporting electrolyte 0.1 M KCl, scan rate 20 mV/s. 0.461% CNF, 0.01 ml PEGDE and 5 ml PEDOT:PSS per 14 ml of polymer dispersion, pumping rate 0.5 ml/h, applied potential 20 kV.

Fibers made by 0.461% CNF polymer dispersions (Fig. 21) exhibited a higher charging capacity than the fibers made by 0.691% CNF dispersion (20 kV 0.5 ml/h) (Fig. 18), but with a similar stability and capacitor like behavior. On the other hand, fibers made by 0.346% CNF polymer dispersion, even though stable, did not have a high charging capacity (Fig 22).

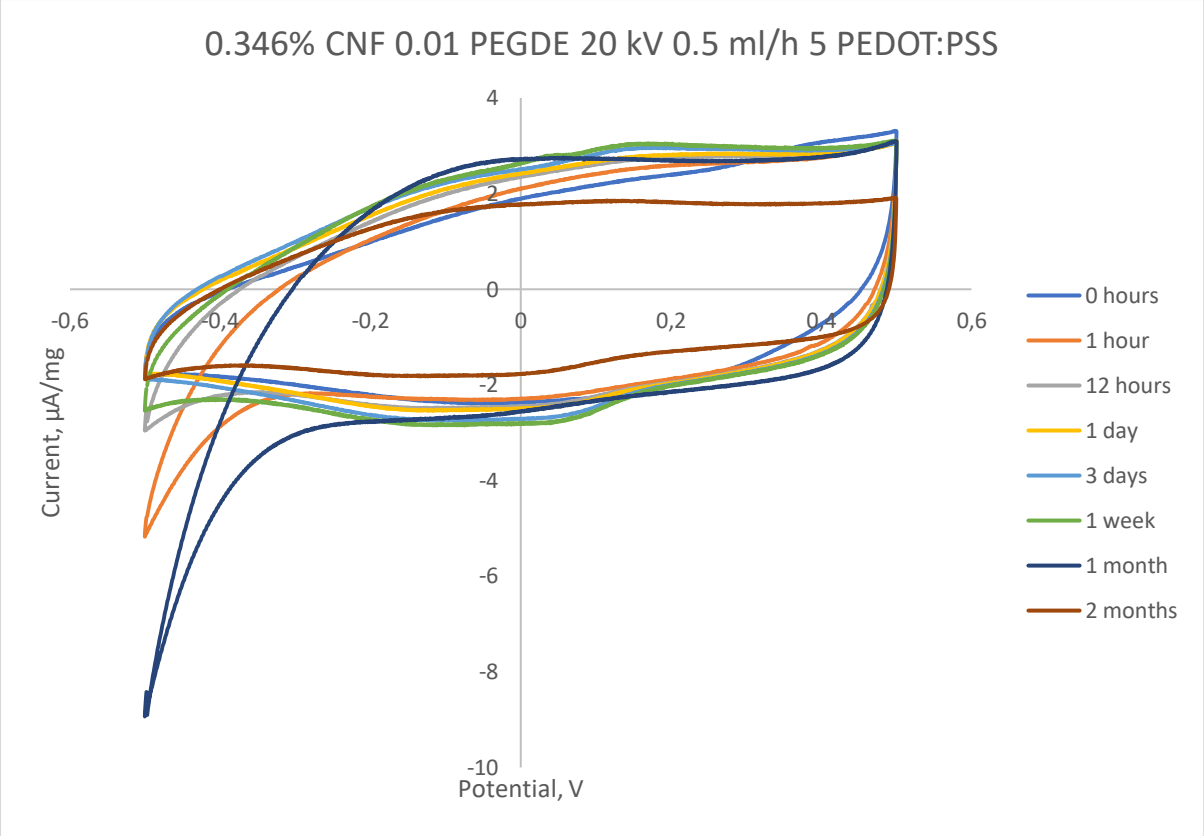

Fig. 22 Long term stability CVs of electrospun nanofibers. Supporting electrolyte 0.1 M KCl, scan rate 20 mV/s. 0.346% CNF, 0.01 ml PEGDE and 5 ml PEDOT:PSS per 14 ml of polymer dispersion, pumping rate 0.5 ml/h, applied potential 20 kV.

The sharp peak that can be observed in Fig. 22 starting a -0.3 V, corresponding to the 1-month measurement, most probably corresponds to oxygen reduction, which could be due to a poor deaeration process during the preparation steps for the CV measurement.

It was observed that the nanofibers had good stability in water, resulting from the presence of PEGDE in the polymer composition. The charging capacities of the nanofibers are similar to those of ideal capacitors. The best charging capacities correspond to nanofibers electrospun from polymer dispersion compositions made from 0.691% CNF, 0.01 ml PEGDE and 5 ml PEDOT:PSS per 14 ml of polymer dispersion, applied potential of 25 kV and pumping rate of 0.6 ml/h and 0.461% CNF, 0.01 ml PEGDE and 5 ml PEDOT:PSS per 14 ml of polymer dispersion, applied potential of 20 kV and 0.5 ml/h. It can be seen in Figs. 18 and 19 that the charging capabilities of the nanofibers depend upon their morphology, which also affects their stability in water, but the morphology has no effect over the initial charging capabilities.

4.2.3. Effect of waiting time before measuring the charging capacity

During the first CV measurements of the fibers spun over the ITO glasses, it was observed that the material experienced a huge increase in its electroactivity after the electrode was exposed to 0.1 M KCl solution for a period of at least 24 h. It was originally believed that this was a behavior characteristic of the material.

The way in which the first measurements were performed consisted of placing the ITO glass with the spun nanofibers in a 0.1 M KCl solution deaerated for 15 min with a flux of N_2 gas, measuring the CV and placing the electrode in a different beaker with 0.1 M KCl until the next measurement. Since there were a lot of fibers being measured sequentially, it often happened that the electrodes due to the 24 h measurements were taken out of the KCl solution one or two hours before the CV was recorded. This resulted in CV's showing a huge increment in the charging capacity of the polymer after being exposed to 0.1 M KCl for at least a day, as it can be observed in Fig. 23.

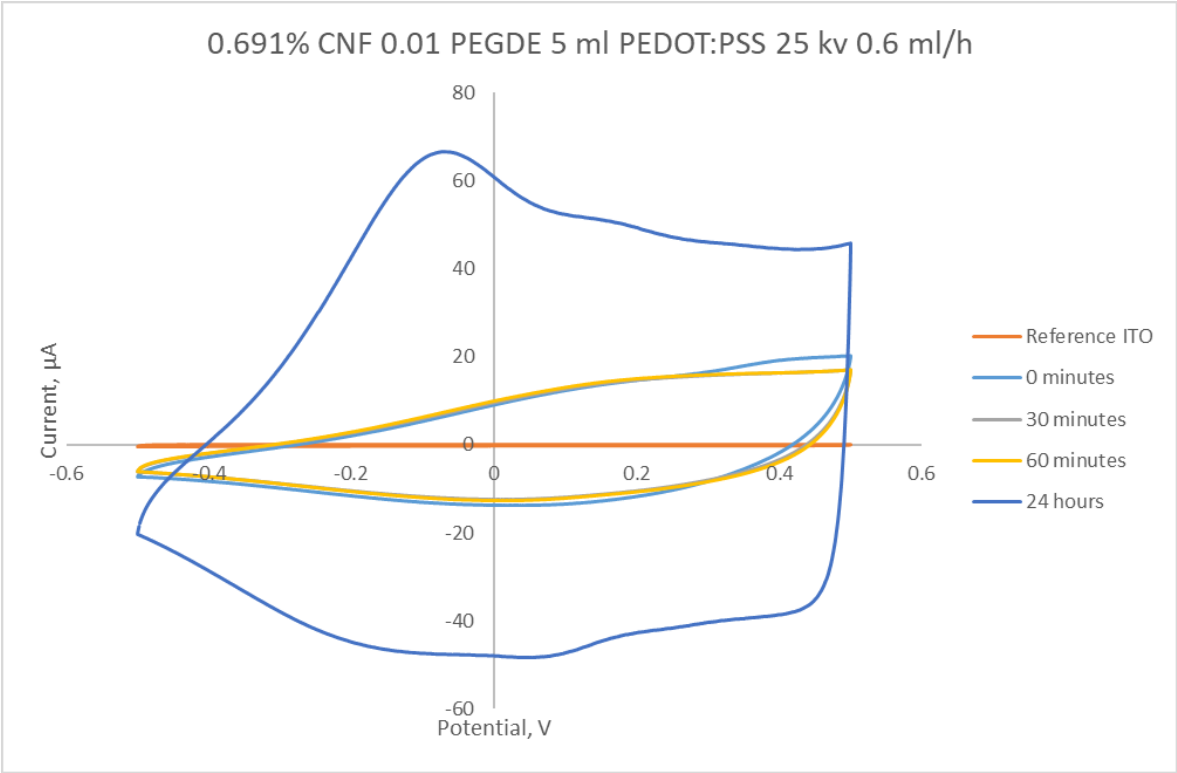

Fig. 23 CVs of electrospun nanofibers made from polymer dispersion composition containing 0.691% CNF, 0.01 ml PEGDE and 5 ml PEDOT:PSS per 14 ml of polymer dispersion, applied potential 25 kV, pumping rate 0.6 ml/h, over ITO glass. Counter electrode: GC. Reference electrode: Ag/AgCl(3 M), scan rate 20 mV/s.

The belief that the material had a huge increase in electroactivity after 24 h of staying in KCl 0.1 M didn't change until the start of the long-term stability measurements. The principal difference between long-term stability measurements and the previous measurements consisted on how long the working electrode was allowed to dry before starting the CV measurement. Since long-term stability measurements were conducted without waiting time before the measurements, the working electrode was never out of the KCl solution for periods longer than 5 minutes, thus not being able to dry. This change in how the working electrode was handled resulted in the lack of huge increase in charging capacity.

Due to how different the voltammograms with drying time looked vs voltammograms of fibers without drying time, it was decided to measure the charging capacities of the polymers, implementing a drying time after a fixed amount of exposure to KCl solution. These measurements were carried out for three days.

6 different fiber compositions were measured during a three day period, in order to observe how drying the electrode before measuring the CV affected the charging capacity of the polymer fibers. All fiber compositions exhibited a capacitor like behavior but a notable difference in the maximum charge achieved during the CV could be observed when compared to the same fiber compositions but measured without a drying period.

Table 7 details the polymer dispersion compositions that were used in the study. All CVs of the polymer dispersion compositions utilized to observe the effect of drying before measuring the CV can be found in appendix B.

Table 7 Polymer dispersion compositions utilized for electrospinning to observe the effect of drying before measuring the CV

CNF, %	PEO 6%, g	PEGDE, ml per 14 ml	Pumping rate, ml/h	Applied potential, kV	PEDOT:PSS, ml per 14 ml	Fiber mass, mg
0.691	7	0.05	0.6	25	5	0.9
0.691	7	0.005	0.6	25	5	0.4
0.691	8	0.01	0.6	25	4	0.2
0	9	0.01	0.5	20	5	1
0	7	0.01	0.5	20	5	1
0.346	7	0.01	0.6	25	5	1

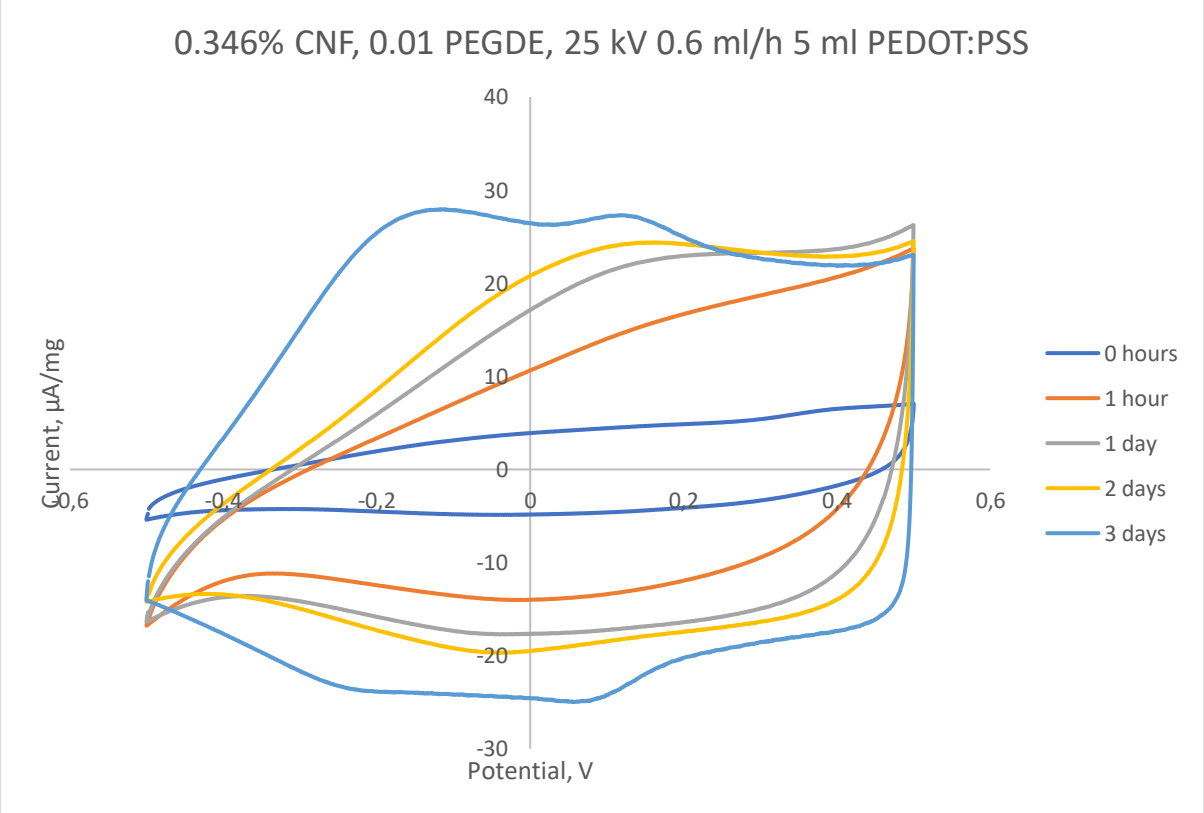

Fig. 24 CVs of electrospun nanofibers with drying time before each measurement cycle. Supporting electrolyte 0.1 M KCl, scan rate 20 mV/s. 0.346% CNF, 0.01 ml PEGDE and 5 ml PEDOT:PSS per 14 ml of polymer dispersion, pumping rate 0.6 ml/h, applied potential 20 kV.

Fig. 24 shows the effect that drying before mesuring the CV had in all the nanofibers studied. A significant increase can be seen, and the shaping of the rectangular box, characteristic of the behavior of the ideal capacitor, can be seen taking shape with the pass of time. It can also be appreciated in Fig. 24 the increase in electrical activity the longer the nanofibers were in contact with the KCl 0.1 M solution.

4.3. Water contact angle

In order to determine the behavior of the nanofibers in respect to water, contact angle studies were carried out. Polymer dispersion compositions used to electrospun nanofibers whose contact angle was studied are listed in Table 8.

All nanofibers studied exhibited a hydrophilic behavior i.e. their water contact angles were less than 90°. This aligns nicely with the expected behavior off the nanofibers. Contact angle measurement images can be seen in Appendix B.

Table 8 Polymer disperion compositions utilized for electrospinning to observe water contact angle

CNF, %	PEGDE, ml per 14 ml	PEDOT:PSS, ml per 14 ml	Applied potential, kV	Pumping rate, ml/h	6wt% PEO, g
0.461	0	4	20	0.5	8
0.461	0.001	4	20	0.5	8
0.461	0.005	4	20	0.5	8
0.461	0.05	4	20	0.5	8
0.691	0	4	20	0.5	8
0.691	0	5	20	0.5	7
0.691	0	4	25	0.6	8
0.691	0	5	25	0.6	7
0.691	0.01	5	20	0.5	7
0.691	0.01	5	25	0.6	7

From the images captured for water contact angle, it can be seen that not a big difference exists in contact angles, since all of them are less than 90º, indicating a hydrophilic behavior. However, a small difference can be appreciated when the nanofibers were spun from polymer dispersion compositions that had a PEGDE content equal or higher to 0.01 ml per 14 ml of polymer dispersion. This behavior supports the addition of PEGDE to the polymer dispersion as a way to provide the nanofiber with a degree of resistivity towards water. A larger concentration of PEGDE may have a more pronounced effect on the contact angle, but this path was not pursued in this thesis, since more PEGDE content in the polymer dispersion made the morphology of the nanofibers worst.

4.4. Infrared spectroscopy

FT-IR measurements were carried out in order to observe possible structural changes in the nanofibers that could be linked to the effect of PEGDE over the fibers. These measurements were also done in order to elucidate the behavior of the nanofiber components after exposure to water.

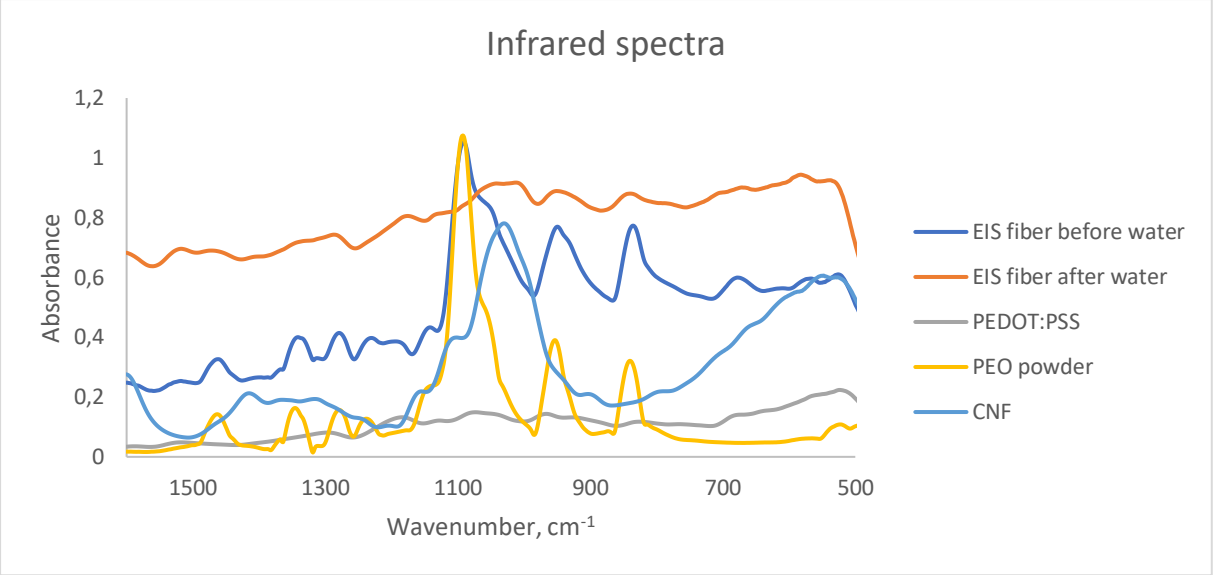

Fig. 25 FT-IR spectra of Electrospun fibers (EIS) before and after contact with water, PEDOT:PSS, PEO powder and CNF 0.691%

In Fig. 25, a broad peak can be seen at around 1100 cm^{-1} in the PEO spectrum (yellow line), followed by two smaller peaks at approximately 950 and 820 cm^{-1}. These three peaks will determine the presence of PEO in the spun fibers, since no other component of the polymer dispersion shares those peaks. CNF presents a broad peak at around 1050 cm^{-1}.

Before contact with water, the electrospun fibers (EIS) exhibits the broad PEO peak and the two smaller peaks that follow it. However, after the EIS was placed in contact with water, the broad PEO peak disappears and the two smaller PEO peaks get noticeable smaller. This data suggests that after exposure with water, PEO dissolves partly from the fibers.

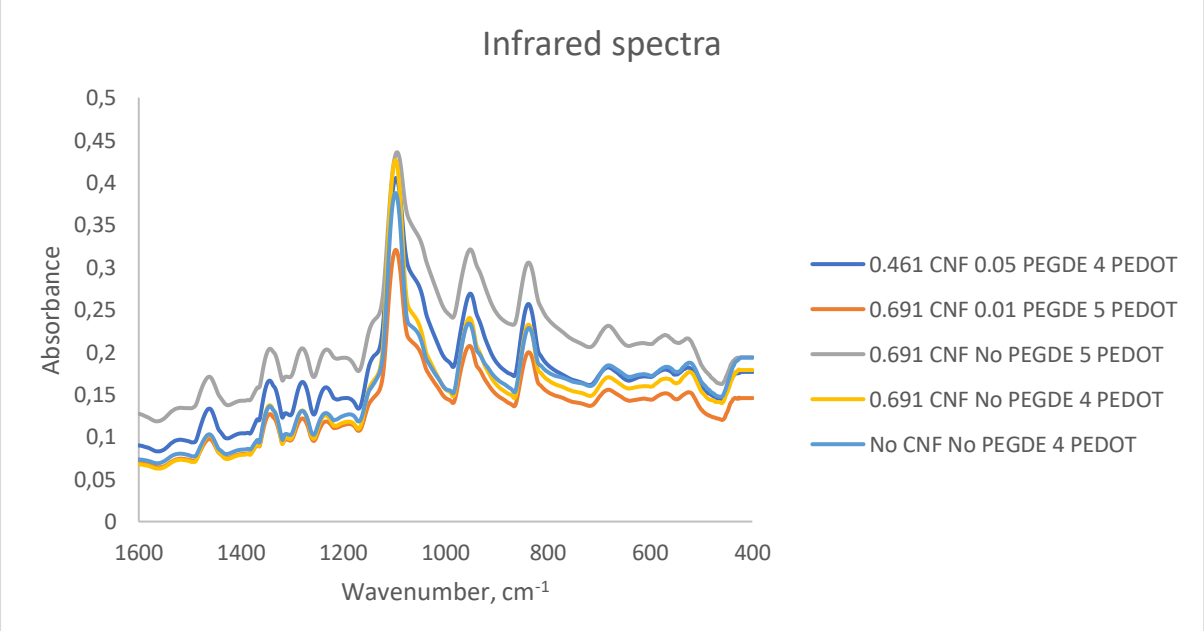

Fig. 26 FT-IR spectra of nanofibers electrospun from different polymer compositions

Fig. 26 shows the spectra of nanofibers spun with different polymer dispersion compositions. The broad peak corresponding to PEO can be appreciated across all compositions. These spectra were measured in order to identify any possible effect PEGDE may have on the structure, but the data shows that the crosslinking can not be evidenced by FT-IR due to many overlapping infrared bands.

4.5. Energy-dispersive X-ray spectroscopy

EDXA measurements were performed to the nanofibers with the best morphology (0.691% CNF, 0.01 PEGDE and 5 ml PEDOT:PSS per 14 ml of polymer dispersion) with applied potentials of 20 and 25 kV and pumping rates of 0.5 and 0.6 ml/h. This was done in order to observe the behavior of PEDOT:PSS when using different electrospinning parameters and the effect of water contact. EDXA data is displayed in Table 9. The sum of C, O, and S percentages will not add up to 100% since the detection of additional elements, mostly impurities, were also detected with EDXA.

Table 9 Nanofibers compositions studied with EDXA

CNF, %	PEGDE, ml per 14 ml	PEDOT:PSS, ml per 14 ml	Applied potential, kV	Pumping rate, ml/h	C, %	O, %	S, %	Water contact?
0.691	0.01	5	20	0.5	50.18	27.15	0.71	No
0.691	0.01	5	25	0.6	51.15	41.95	1.61	No
0.691	0.01	5	25	0.6	33.98	14.8	1.97	Yes

As ti could be shown by FT-IR measurements that PEO was slightly dissolving from the nanofibers during contact with water, EDXA was performed to confirm whether only PEO was dissolving or if other components of the polymer composition were dissolving too. It can be seen from the data in Table 9 that the carbon percentage reduces its value in almost half. Sulfur percentage, on the other hand, doesn't experience a significant change, which could mean that PEDOT:PSS is being crosslinked by PEGDE more efficiently to the CNF than PEO is.

When comparing the nanofibers spun with an applied potential of 20 kV to those spun with 25 kV, it is clear that the PEDOT:PSS content (signalized by the sulfur percentage) is higher when the fibers where spun under a higher applied potential. This result implies that integration between the components of the polymer dispersion is more efficient at a higher voltage, which also relates to the CV's results that show higher stability in water for nanofibers spun with 25 kV of applied voltage (Figs.18 and 19).

5. Conclusions

A series of novel polymer dispersion compositions containing cellulose nanofibrils and PEDOT:PSS together with PEO were prepared for electrospinning. PEGDE was used in order to crosslink the structure and induce water resistivity to the fibers. The best electrospinning parameters were identified for these polymer compositions, based on

the morphology of the nanofibers studied with SEM and electroactivity studied by cyclic voltammetry. The best morphology was determined based on the fiber appearance and presence of imperfections in the structure, i.e. beads or blobs. It was observed that both the fiber morphology and electroactivity were heavily dependent upon electrospinning parameters.

The best nanofiber morphology across the polymer dispersion compositions studied in this work was found to be that corresponding to a polymer dispersion containing 2 g of 0.691% CNF, 7 g of 6wt% PEO, 5 ml of PEDOT:PSS and 0.01 ml of PEGDE per 14 ml of polymer dispersion, electrospun with an applied voltage of 25 kV and a pumping rate of 0.6 ml/h. The effect of the distance to the collector plate was observed to have a minor effect on the electrospinning process and 15 cm was found to be an optimal distance.

Cyclic voltammetric experiments were performed in order to observe the electrical capabilities of the electrospun nanofibers. Stability tests in water were also performed by CV and the changes in the electrical activity monitored. It was found that the electrospun fibers are stable in water without signs of decay in their electrical activity for up to two months. The electrical capabilities of all the fibers studied was found to be similar to the behavior of an ideal capacitor. It was observed that the electrical capabilities of the fibers experienced a huge increment if the nanofibers were submerged in water and allowed to dry before measuring the CV's. This increment in electrical activity could be related to the dissolution of PEO present in the nanofibers after exposure to water and rearrangement of the PEDOT:PSS chain-like structure. Similarly, it was noticed that the stability in water and the electroactivity of the nanofibers benefited from having a higher content of CNF in the polymer dispersion used to electrospun the nanofibers.

Water contact angle measurements were carried out in order to determine the hydrophobicity or hydrophilicity of the nanofibers. All the nanofiber compositions measured exhibited contact angles lower than 90° which correspond to a hydrophilic behavior. It was observed that addition of increased amounts of PEGDE to the polymer composition did not change the hydrophilic behavior, but altered it by a slight margin, suggesting that PEGDE is crosslinking the structure of the nanofibers.

In order to determine the interaction between PEGDE and the components of the polymer dispersion, FT-IR measurements were performed. No conclusion could be attained by FT-IR measurements due to many overlapping broad bands from PEO CNF, and PEDOT:PSS. FT-IR spectroscopy was useful to determine the behavior of the nanofiber's components after water exposure. A decline of the PEO band absorbance at around 1100cm^{-1} was observed after the nanofibers were exposed to water, suggesting that a part of PEO dissolves from the structure after water exposure. It was also observed with SEM that after water exposure, the nanofibers almost doubled their diameter while loosing a part of their thread structure, which could be related to the dissolution of PEO.

It was also observed by EDXA that after water exposure, the carbon content in the nanofibers diminished by almost half of its original value, while no noticeable

difference was found with in the sulfur content, which indicated the presence of PEDOT:PSS in the fibers.

Overall, the electrospinning of water-resistant nanofibers from a novel polymer dispersion containing nanocellulose and the conducting polymer PEDOT:PSS possessing electrical activity, high stability and good morphology was achieved.

6. References

1. Cheng C., Li X., Yu X., Wang M. & Wang X. (2019) Chapter 14: Electrospun nanofibers for water treatment. In Ding B., Wang X. & Yu J. (Eds.), *Electrospinning: Nanofabrication and applications.* doi: 10.1016/B978-0-323-51270-1.00014-5

2. Li L., Peng S., Lee J.K.Y., Ji D., Srinivasan M. & Ramakrishna S. (2017) Electrospun hollow nanofibers for advanced secondary batteries. *Nano Energy, 39,* 111 – 139. doi: 10.1016/j.nanoen.2017.06.050

3. Li Y., Abedalwafa M.A., Tang L., Li D. & Wang L. (2019) Chapter 18: Electrospun nanofibers for sensors. In Ding B., Wang X. & Yu. J (Eds.), *Electrospinning: Nanofabrication and applications.* doi: 10.1016/B978-0-323-51270-1.00018-2

4. Zhai Y., Liu H., Li L., Yu J. & Ding B. (2019) Chapter 22: Electrospun nanofibers for Lithium-Ion batteries. In Ding B., Wang X. & Yu. J (Eds.), *Electrospinning: Nanofabrication and applications.* doi: 10.1016/B978-0-323-51270-1.00022-4

5. Asmatulu R. & Khan W.S. (2019) Chapter 8: Electrospun nanofibers for catalyst applications. In Asmatulu R. & Khan W.S. (Eds.), *Synthesis and applications of Electrospun nanofibers*. doi: 10.1016/B978-0-12-813914-1.00008-0

6. Liu M., Duan X.P., Li Y.M., Yang D.P. & Long Y.Z. (2017) Electrospun nanofibers for wound healing. *Material Science and Engineering: C, 76,* 1413 – 1423. doi: 10.1016/j.msec.2017.03.034

7. Norouzi M. (2018) Recent advances in brain tumor therapy: application of electrospun nanofibers. *Drug DiscoveryTtoday, 23(4),* 912 – 919. doi: 10.1016/j.drudis.2018.02.007

8. Bhardwaj N. & Kundu S.C. (2010) Electrospinning: A fascinating fiber fabrication technique. *Biotechnology Advances, 28,* 325 – 347. doi: 10.1016/j.biotechadv.2010.01.004

9. Agarwal S., Greiner A. & Wendorff J.H. (2013) Functional materials by electrospinning of polymers. *Progress in Polymer Science, 38,* 963 – 991. doi: 10.1016/j.progpolymsci.2013.02.001

10. Okuzaki H., Harashina Y. & Yan H. (2009) Highly conductive PEDOT/PSS microfibers fabricated by wet-spinning and dip-treatment in ethylene glycol. *European Polymer Journal, 45,* 256 – 261. doi: 10.1016/j.eurpolymj.2008.10.027

11. Pisuchpen t., Keaw-on N., Kitikulvarakorn K., Kusonsong S., Sritana-anant Y., Supaphol P. & Hoven V.P. (2017) Electrospinning and solid state polymerization: A simple and versatile route to conducting PEDOT composite films. *European Polymer Journal, 96,* 452 – 462. doi: 10.1016/j.eurpolymj.2017.09.033

12. Dinesh V.P., Sriram Kumar R., Sukhananazerin A., Sneha J.M., Kumar P.M. & Biji P. (2019) Novel stainless steel based, eco-friendly dye-sensitized solar cells using electrospun porous ZnO nanofibers. *Nano-structures & Nano-objects, 19,* 100311. doi: 10.1016/j.nanoso.2019.100311

13. Motlak M., Hamza A.M., Hammed M.G. & Barakat N.A.M. (2019) Cd-doped TiO_2 nanofibers as effective working electrode for the dye sensitized solar cells. *Material letters, 246,* 206 – 209. doi: 10.1016/j.matlet.2019.03.067

14. Unnithan A.R., Arathyram R.S. & Kim C.S. (2015) Chapter 3 – Electrospinning of Polymers for Tissue engineering. In Thomas S., Grohens Y. & Ninan N. (Eds.), *Nanotechnology applications for tissue engineering.* doi: 10.1016/B978-0-323-32889-0.00003-0

15. Nasir M., Subhan A., Prihandoko B. & Lestariningsih T. (2017) Nanostructure and property of electrospun SiO_2-cellulose acetate nanofiber composite by electrospinning. *Energy Procedia, 107,* 227 – 231. doi: 10.1016/j.egypro.2016.12.133

16. Si J., Cui Z., Wang Q., Liu Q. & Liu C. (2016) Biomietic composite scaffolds based on mineralization of hydroxyapatite on electrospun poly(ε-caprolactone)/nanocellulose fibers. *Carbohydrate Polymers, 143,* 270 – 278. doi: 10.1016/j.carbpol.2016.02.015

17. Kargarzadeh H., Mariano M., Huang J., Lin N., Ahmad I., Dufresne A. & Thomas S. (2017) Recent developments on nanocellulose reinforce polymer nanocomposites: A review. *Polymer, 132,* 368 – 393. doi: 10.1016/j.polymer.2017.09.043

18. Abitbol T., Rivkin A., Cao Y., Nevo Y., Abraham E., Ben-Shalom T., Lapidot S. & Shoseyov O. (2016) Nanocellulose, a tiny fiber with huge applications. *Current opinion in biotechnology, 39,* 76 – 88. doi: 10.1016/j.copbio.2016.01.002

19. Zhang K., Li Z., Kang W., Deng N., Yan J., Ju J., Liu Y. & Cheng B. (2018) Preparation and characterization of tree-like cellulose annofiber membranes via the electrospinning method. *Carbohydrate polymers, 183,* 62 – 69. doi: 10.1016/j.carbpol.2017.11.032

20. Hersel U., Dahmen C. & Kessler H. (2003) RGD modified polymers: biomaterials for stimulated cell adhesion and beyond. *Biomaterials, 24(24),* 4385 – 4415. doi: 10.1016/S0142-9612(03)00343-0

21. Torgbo S. & Sukyai P. (2018) Bacterial cellulose-based scaffold materials for bone tissue engineering. *Applied materials today, 11,* 34 – 49. doi: 10.1016/j.apmt.2018.01.004

22. Liu R., Ma L., Mei J., Huang S., Yang S., Li E. & Yuan G. (2017) Large areal mass, mechanically though and freestanding electrode based on heteroatom-doped carbon nanofibers for flexible supercapacitors. *Chemistry a European journal, 23(11),* 2610 – 2618. doi: 10.1002/chem.201604535

23. Hoeng F., Denneulin A. & Bras J. (2016) Use of nanocellulose in printed electronics: a review. *Nanoscale, 8(27),* 13131 – 13154. doi: 10.1039/C6NR03054H

24. Phantong P., Reubroycharoen P., Hao X., Xu G., Abudula A. & Guan G. (2018) Nanocellulose: Extraction and application. *Carbon resources conversion, 1(1),* 32 – 43. doi: 10.1016/j.crcon.2018.05.004

25. Awuzie C.I. (2017) Conducting polymers. *Materials today: Proceedings, 4(4),* 5721 – 5726. doi: 10.1016/j.matpr.2017.06.036

26. Zarrin N., Tavanai H., Abdolmaleki A., Bazarganipour M. & Alihosseini F. (2018) An investigation on the fabrication of conductive polyethylene dioxythiophene (PEDOT) nanofibers through electrospinning. *Synthetic metals, 244,* 143 – 149. doi: 10.1016/j.synthmet.2018.07.013

27. Tian Q., Xu J., Zuo Y., Li Y., Zhang J., Zhou Y., Duan X., Lu L., Jia H., Xu Q. & Yu Y. (2019) Three-dimensional PEDOT composite based electrochemical sensor for sensitive detection of chlorophenol. *Journal of electrical chemistry, 837,* 1 – 9. doi: 10.1016/j.jelechem.2019.01.055

28. Zhuzhelskii D.V., Tolstopjatova E.G., Eliseeva S.N., Ivanov A.V., Miao S. & Kondratiev V.V. (2019) Electrochemical properties of PEDOT/WO_3 composite films for high performance supercapacitor application. *Electrochimica Acta, 299,* 182 – 190. doi: 10.1016/j.electacta.2019.01.007

29. Yu J.H. & Rutledge G.C. (2007) Electrospinning. In John Wiley & Sons (Eds.), *Encyclopedia of polymer science and technology.* doi: 10.1002/0471440264.pst554

30. Huang Z.M., Zhang Y.Z., Kotaki M. & Ramakrishna S. (2003) A review on polymer nanofibers by electrospinning and their applications in nanocomposites. *Composites science and technology, 63(15),* 2223 – 2253. doi: 10.1016/S0266-3538(03)00178-7

31. Daristotle J.L., Behrens A.M., Sandler A.D. & Kofinas P. (2016) A review of the fundamental principles and applications of solution blow spinning. *ACS applied materials & interfaces, 8(51),* 34951 – 34963. doi: 10.1021/acsami.6b12994

32. Vazquez B., Vasquez H. & Lozano K. (2012) Preparation and characterization of polyvinylidene fluoride nanofibrous membranes by forcespinning™. *Polymer engineering and science, 52(10),* 2260 – 2265. doi: 10.1002/pen.23169

33. Bai X., Liao S., Huang Y., Song J., Liu Z., Fang M., Xu C., Cui Y. & Wu H. (2017) Continuous draw spinning of extra-long silver submicron fibers with micrometer patterning capability. *Nano letters, 17(3),* 1883 – 1891. doi: 10.1021/acs.nanolett.6b05205

34. Paramonov S.E., Jun H-W. & Hartgerink J.D. (2006) Self-assembly of peptide-amphiphile nanofibers: The role of hydrogen bonding and amphiphilic packing. *Journal of the American Chemical Society, 128(22),* 7291 – 7298. doi: 10.1021/ja060573x

35. Lee J., Lee P., Lee H., Lee D., Lee S.S. & Ko S.H. (2012) Very long Ag nanowire synthesis and its application in a highly transparent, conductive and flexible metal electrode touch panel. *Nanoscale, 4,* 6408 – 6414. doi: 10.1039/C2NR31254A

36. Li D. & Xia Y. (2004) Electrospinning of nanofibers: reinventing the wheel? *Advanced materials, 16(14),* 1151 – 1170. doi: 10.1002/adma.200400719

37. Jiang H., Fang D., Hsiao B.S., Chu B. & Chen W. (2004) Optimization and characterization of Dextran Membranes prepared by electrospinning. *Biomacromolecules, 5(2),* 326 – 333. doi: 10.1021/bm034345w

38. Huang L., Nagapudi K., Apkarian R.P. & Chaikof E.L. (2001) Engineered collagen-PEO nanofibers and fabrics. *Journal of biomaterials science, polymer edition, 12(9),* 979 – 993. doi: 10.1163/156856201753252516

39. Kim B., Park H., Lee S.H. & Sigmund W.M. (2005) Poly(acrylic acid) nanofiber by electrospinning. *Materials letters, 59(7),* 829 – 832. doi: 10.1016/j.matlet.2004.11.032

40. Son W.K., Youk J.H., Lee T.S. & Park W.H. (2004) The effects of solution properties and polyelectrolyte on electrospinning of ultrafine poly(ethylene oxide) fibers. *Polymer, 45(9),* 2959 – 2966. doi: 10.1016/j.polymer.2004.03.006

41. Demir M.M., Yilgor I., Yilgor E. & Erman B. (2002) Electrospinning of polyurethane fibers. *Polymer, 43(11),* 3303 – 3309. doi: 10.1016/S0032-3861(02)00136-2

42. Zhao Z., Li J., Yuan X., Li X., Zhang Y. & Sheng J. (2005) Preparation and properties of electrospun poly(vinylidene fluoride) membranes. *Journal of applied polymer science, 92(2),* 466 – 474. doi: 10.1002/app.21762

43. Massaglia G. & Quaglio M. (2018) Semiconducting nanofibers in photoelectrochemistry. *Materials science in semiconductor processing, 73,* 13 – 21. doi: 10.1016/j.mssp.2017.06.047

44. Tokura S., Tamura H., Takai M., Higuchi T. & Asano H. (2000) Continuous harvest of cellulosic filament during cultivation of *Acetobacter Xylinum*. In Kennedy J.F., Phillips G.O. & Williams P.A. (Eds.), *Cellulosic pulps, fibres and materials* (pp. 3 – 12). Abington, Cambridge: Woodhead Publishing Ltd.

45. Wertz J.L., Bédué O. & Mercier J.P. (2010) Perspectives. In *Cellulose science and technology* (p. 334). Boca Raton, Fl: CRC Press.

46.Wertz J.L., Bédué O. & Mercier J.P. (2010) structure and properties of cellulose. In *Cellulose science and technology* (pp. 130 – 140). Boca Raton, Fl: CRC Press.

47. Klemm D., Cranston E.D., Fischer D., Gama M., Kedzior S.A., Kralisch D., Lramer F., Kondo T., Lindström T., Nietzsche S., Petzold-Welcke K. & Rauchfuß F. (2018) Nanocellulose as a natural source for groundbreaking applications in materials science: Today's state. *Materials today, 21(7),* 720 – 748. doi: 10.1016/j.mattod.2018.02.001

48. Sabo R., Yermakov A., Law C.T. & Elhajjar R. (2016) Nanocellulose-enabled electronics, energy harvesting devices, smart materials and sensors: A review. *Journal of renewable materials, 4(5),* 297 – 312. doi: 10.7569/JRM.2016.634114

49. Klemm D., Krammer F., Moritz S., Lindström T., Ankerfors M., Gray D. & Dorris A. (2011) Nanocelluloses: A new family of Nature-based materials. *Angewandte chemie international edition, 50(24),* 5438 – 5466. doi: 10.1002/anie.201001273

50. Du X., Zhang Z., Liu W. & Deng Y. (2017) Nanocellulose-based conductive materials and their emerging applications in energy devices – a review. *Nano energy, 35,* 299 – 320. doi: 10.1016/j.nanoen.2017.04.001

51. Carpenter A.W., de Lannoy C.F. & Wiesner M.R. (2015) Cellulose nanomaterials in water treatment technologies. *Environmental science and technology, 49(9),* 5277 – 5287. doi: 10.1021/es506351r

52. Ladhar A., Arous M., Kaddami H., Raihane M., Kallel A., Graça M.P.F. & Costa L.C. (2015) AC and DC electrical conductivity in natural rubber/nanofibrillated cellulose nanocomposites. *Journal of molecular liquids, 209,* 272 – 279. doi: 10.1016/j.molliq.2015.04.020

53. Bochek A.M. (2003) Effect of hydrogen bonding on cellulose solubility in aqueous and nonaqueous solvents. *Russian journal of applied chemistry, 76(11),* 1711 – 1719. doi: 10.1023/B:RJAC.0000018669.88546.56

54. Wertz J.L., Bédué O. & Mercier J.P. (2010) Swelling and dissolution of cellulose. In Wertz J.L., Bédué O. & Mercier J.P. (Eds.), Cellulose science and technology (pp. 148 – 149). Boca Raton, Fl: CRC Press.

55. Thielemans W., Babacar L., Dufresne A. & Belgacem N. (2007, April 26th) *Cellulose and starch reinforced composites and nanocomposites*. Retrieved from http://cerig.pagora.grenoble-inp.fr//dossier/LGP2-scientific-report/page20.htm

56. Fortunato G., Zimmerman T., Lübben J., Bordeanu N. & Hufenus R. (2012) Reinforcement of polymeric submicrometer-sized fibers by microfibrillated cellulose. *Macromolecular materials and engineering, 297(6),* 576 – 584. doi: 10.1002/mame.201100408

57. Zarrin N., Tavannai H., Abdolmaleki A., Bazarganipour M. & Alihosseini F. (2018) An investigation on the fabrication of conductive polyethylene dioxythiophene (PEDOT) nanofibers through electrospinning. *Synthetic metals, 244,* 143 – 149. doi: 10.1016/j.synthmet.2018.07.013

58. Peymanfar R., Norouzi F. & Javanshir S. (2019) Preparation and characterization of one-pot PANi/Fe/Fe_3O_4/Fe_2O_3 nanocomposite and investigation of its microwave, magnetic and optical performance. *Synthetic metals, 252,* 40 – 49. doi: 10.1016/j.synthmet.2019.04.008

59. Kulkarni, S., Patil P., Mujumdar A. & Naik J. (2018) Synthesis and evaluation of gas sensing properties of PANI, PANI/SnO_2 and PANI/SnO_2/rGO nanocomposites at room temperature. *Inorganic chemistry communications, 96,* 90 – 96. doi: 10.1016/j.inoche.2018.08.008

60. Baldissera A.F., da Silva Silveira M.R., Beraldo C.H., Tocchetto N.S. & Ferreira C.A. (2019) Polymeric organic coating based on PANI-ES and PANI-ES/APP for fire protection. *Journal of materials research and technology.* doi: 10.1016/j.jmrt.2019.04.022

61. Chen Y., Zhang X., Xu C. & Xu H. (2019) The fabrication of asymmetry supercapacitor based on MWCNTs/MnO_2/PPy composites. *Electrochimica acta, 309,* 424 – 431. doi: 10.1016/j.electacta.2019.04.072

62. Song X., Mei J., Ye G., Wang L., Ananth A., Yu L. & Qiu X. (2019) *In situ* pPy-modification of chitosan porous membrane from mussel shell as a cardiac patch to

repair myocardial infarction. *Applied materials today, 15,* 87 – 99. doi: 10.1016/j.apmt.2019.01.003

63. Silvestri S., Ferreira C.D., Oliveira V., Varejão J.M.T.B., Labrincha J.A. & Tobaldi D.V. (2019) Synthesis of PPy-ZnO composite used as photocatalyst for the degradation of diclofenac under simulated solar irradiation. *Journal of photochemistry and photobiology A: chemistry, 375,* 261 – 269. doi: 10.1016/j.jphotochem.2019.02.034

64. Kankare J. (1998) Electronically conducting polymers: Basic methods of synthesis and characterization. In Wise D.L., Waek G.E., Trantolo D.J., Looper T.M. & Gresser J.D. (Eds.), *Electrical and optical polymer systems* (pp.167 – 199). New York, NY: Marcel Dekker, Inc.

65. Aasmundtveit K.E., Samuelsen E.J., Inganäs O., Pettersson L.A.A., Johansson T. & Ferrer S. (2000) Structural aspects of electrochemical doping and dedoping of poly(3,4-ethylenedioxythiphene). *Synthetic metals, 113(1-2),* 93 – 97. doi: 10.1016/S0379-6779(00)00181-8

66. Henning, S. & Adhikari R. (2017) Scanning electron microscopy, ESEM, and X-ray microanalysis. In Thomas S., Thomas R., Zachariah A.K. & Mishra R.K., *Microscopy methods in nanomaterials characterization* (pp. 2 – 15). doi: 10.1016/B978-0-323-46141-2.00001-8

67. Michler G.H. (2008) Scanning electron microscopy (SEM). In Pash H. (Ed.), *Electron microscopy of polymers* (pp. 88 – 94). doi: 10.1007/978-3-540-36352-1

68. Mishra R.K., Zachariah A.K. & Thomas S. (2017) Energy dispersive X-ray spectroscopy techniques for nanomaterial. In Thomas S., Thomas R., Zachariah A.K. & Mishra R.K., *Microscopy methods in nanomaterials characterization* (pp. 383 – 405). doi: 10.1016/B978-0-323-46141-2.00012-2

69. Michler G.H. (2008) Scanning electron microscopy (SEM). In Pash H. (Ed.), *Electron microscopy of polymers* (pp. 105 – 115). doi: 10.1007/978-3-540-36352-1

70. Southampton Electrochemistry Group (1993) Potential sweep techniques and cyclic voltammetry. In *Instrumental Methods in electrochemistry*, (pp. 178 – 228). Chichester, West Sussex: Ellis Horwood Ltd.

71. Nakamoto, K. (2009) Theory of normal vibrations. In *Infrared and Raman spectra of inorganic and coordination compounds. Part A.* (p. 29). Hoboken, NJ: John Wiley & Sons, Inc.

72. Subramanian A. & Rodriguez-Saona L. (2009) Fourier Transformed Infrared (FTIR) spectroscopy. In Sun D.W. (Ed.), *Infrared spectroscopy for food quality analysis and control,* (p. 169). doi: 10.1016/B978-0-12-374136-3.00007-9

73. Renner G., Schmidt T.C. & Schram J. (2017) Characterization and quantification of microplastics by infrared spectroscopy. In Rocha-Santos T.A.P. & Duarte A. (Eds.), *Characterization and analysis of microplastics,* (p. 20). doi: 10.1016/bs.coac.2016.10.006

74. Förch R., Schönherr H. & Jenkins A.T.A. (2009) Appendix C: Contact Angle Goniometry. In *Surface design: Applications in bioscience and nanotechnology* (p. 471). doi: 10.1002/9783527628599

Image references

Fig 1. Li D. & Xia Y. (2004) Electrospinning of nanofibers: reinventing the wheel? *Advanced materials, 16(14),* 1151 – 1170. doi: 10.1002/adma.2004007194

Fig 2. Aabloo A., French A.D. & Mikelsaar R.H. (1995) Packing energy calculations on the crystalline structure of cellulose I. In Kennedy J.F., Phillips G.O. & Williams P.A. (Eds.), *Cellulose and cellulose derivatives,* (p. 53). doi: 10.1533/9781845698539.2.49

Fig 3. Michler G.H. (2008) Scanning electron microscopy (SEM). In Pash H. (Ed.), Electron microscopy of polymers (pp. 106). doi: 10.1007/978-3-540-36352-1

Fig 5. Förch R., Schönherr H. & Jenkins A.T.A. (2009) Appendix C: Contact Angle Goniometry. In Surface design: Applications in bioscience and nanotechnology (p. 471). doi: 10.1002/9783527628599

7. Appendixes

7.1. Appendix A

CVs of nanofibers made from polymer dispersion compositions containing 4 ml PEDOT:PSS per 14 ml of polymer dispersion

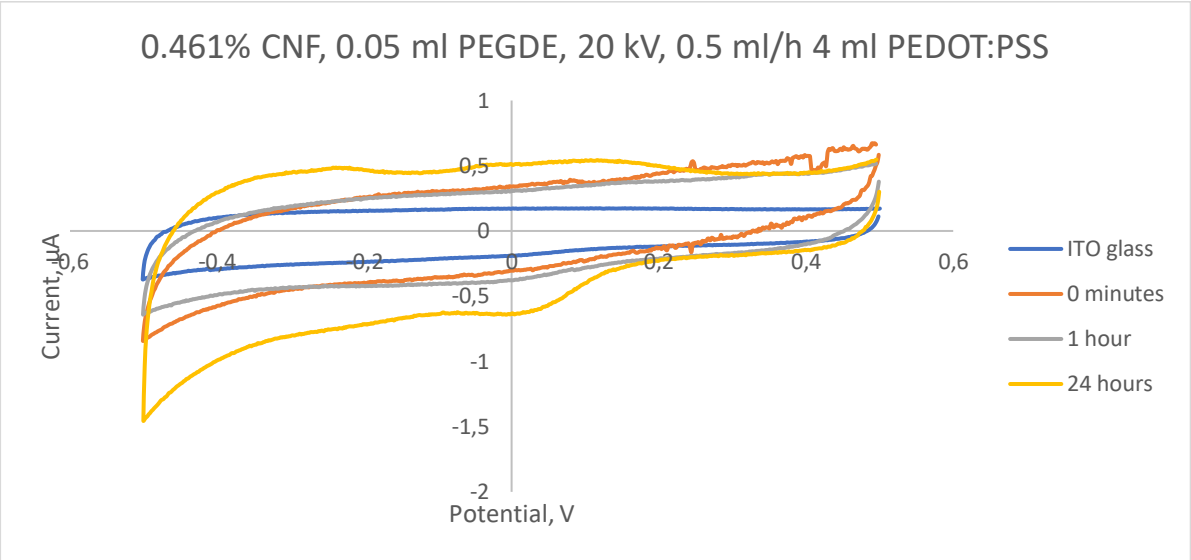

Nanofibers electrospun from polymer dispersion composition made with 0.461% CNF, 0.05 ml PEGDE and 4 ml PEDOT:PSS per 14 ml of polymer dispersion, applied potential 20 kV, pumping rate 0.5 ml/h. Supporting electrolyte KCl 0.1 M, scan rate 20 mV/s

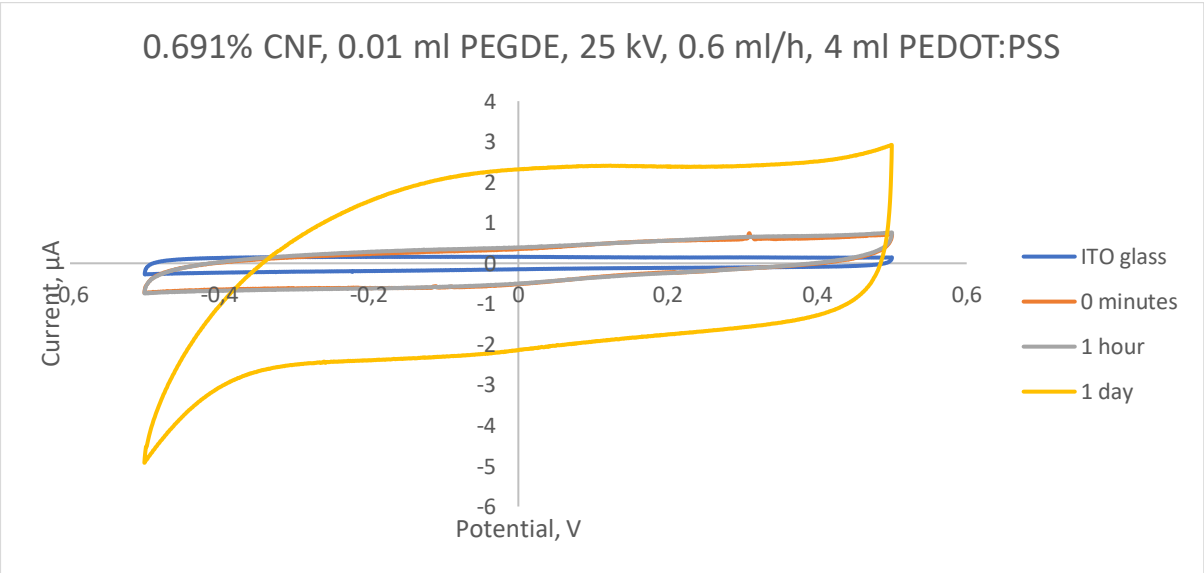

Nanofibers electrospun from polymer dispersion composition made with 0.691% CNF, 0.01 ml PEGDE and 4 ml PEDOT:PSS per 14 ml of polymer dispersion, applied potential 25 kV, pumping rate 0.6 ml/h. Supporting electrolyte KCl 0.1 M, scan rate 20 mV/s

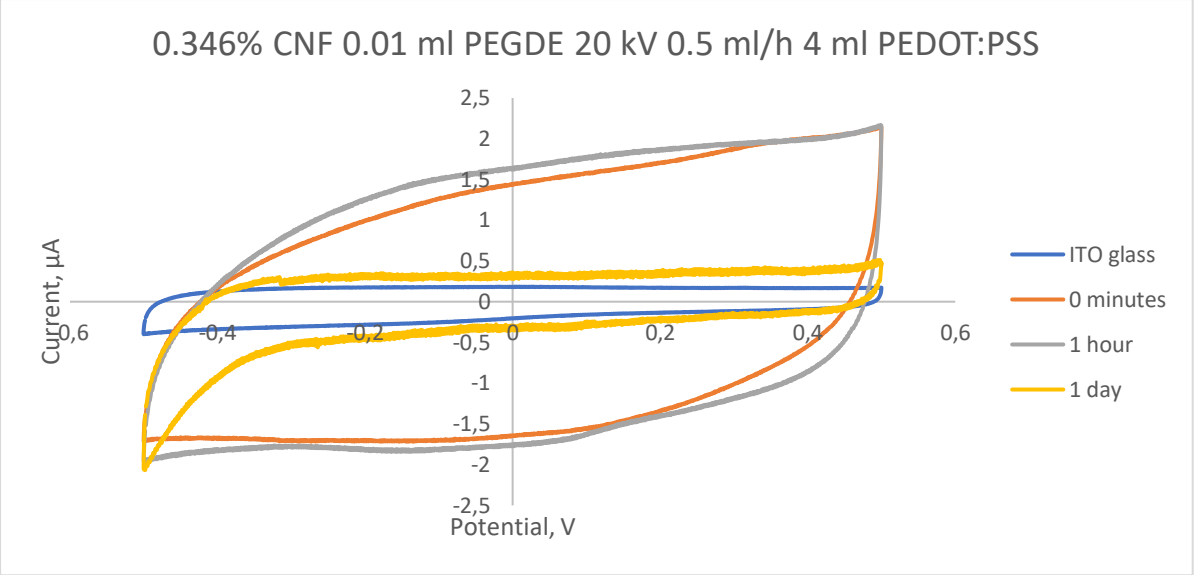

Nanofibers electrospun from polymer dispersion composition made with 0.346% CNF, 0.01 ml PEGDE and 4 ml PEDOT:PSS per 14 ml of polymer dispersion, applied potential 20 kV, pumping rate 0.5 ml/h. Supporting electrolyte KCl 0.1 M, scan rate 20 mV/s

7.2. Appendix B

CVs of nanofibers used to observe the effect of drying before measuring charging capacity

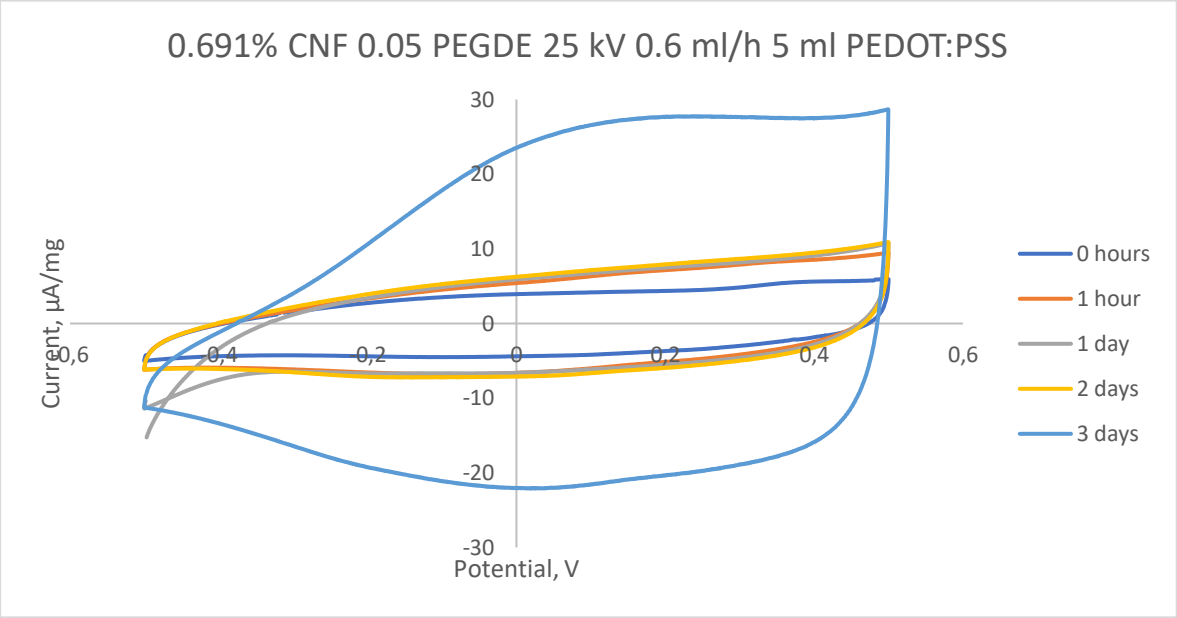

Nanofibers electrospun from polymer dispersion made with 0.691% CNF, 0.05 ml PEGDE and 5 ml PEDOT:PSS per 14 ml of polymer dispersion, applied potential 25 kV, pumping rate 0.6 ml/h. Supporting electrolyte KCl 0.1 M, scan rate 20 mV/s

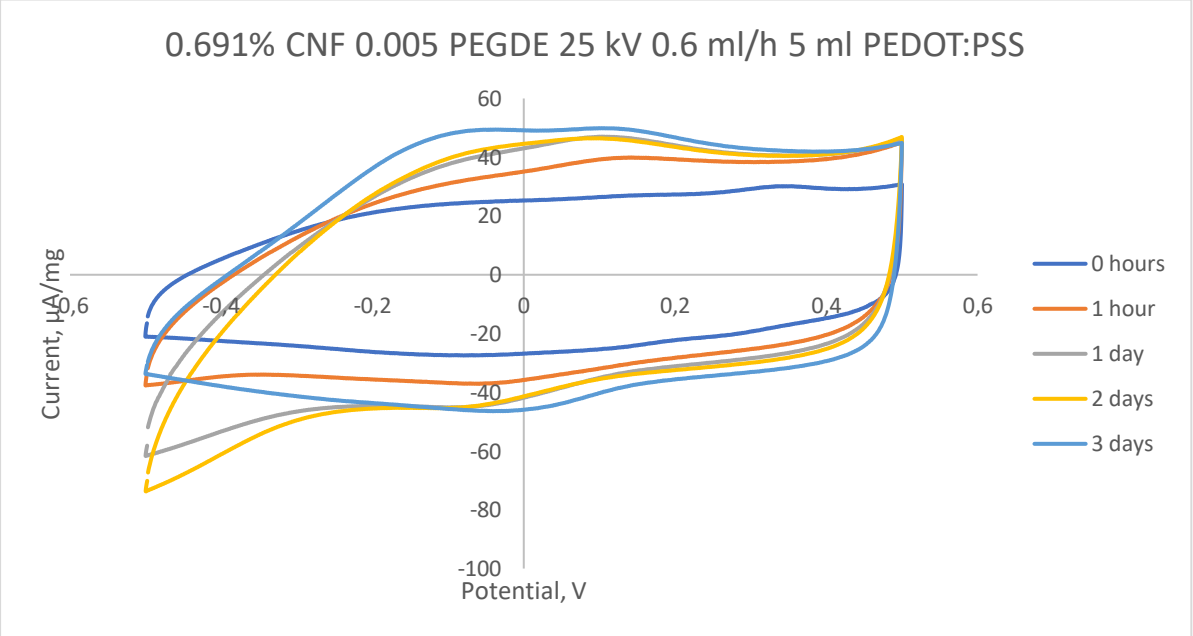

Nanofibers electrospun from polymer dispersion made with 0.691% CNF, 0.005 ml PEGDE and 5 ml PEDOT:PSS per 14 ml of polymer dispersion, applied potential 25 kV, pumping rate 0.6 ml/h. Supporting electrolyte KCl 0.1 M, scan rate 20 mV/s

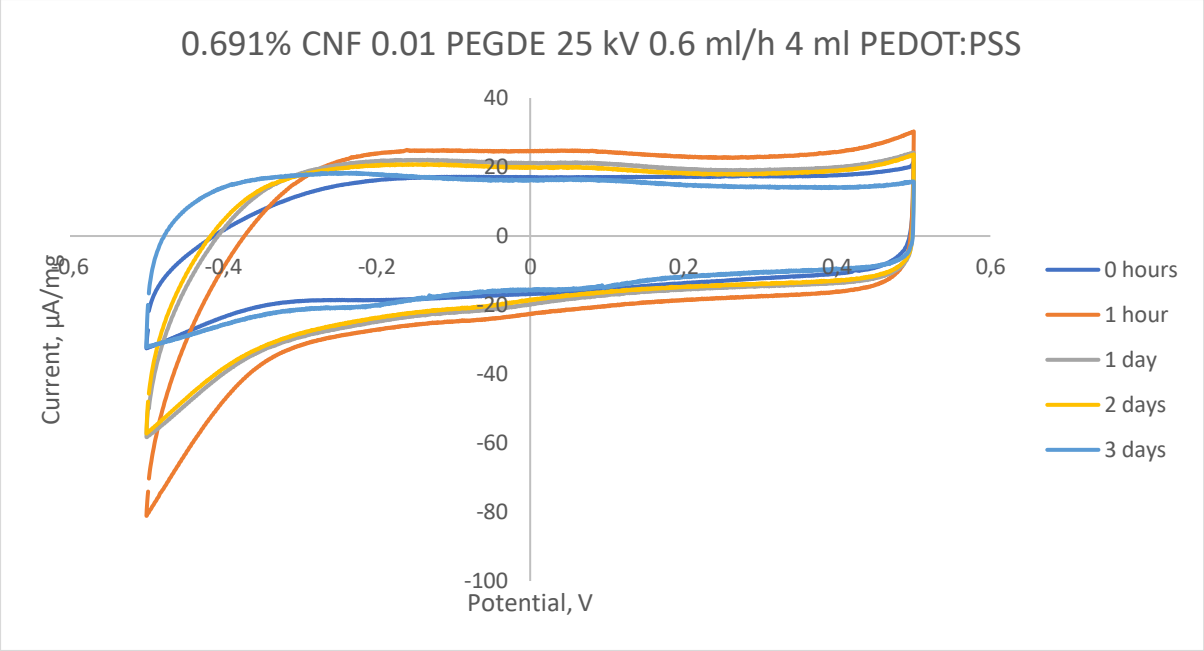

Nanofibers electrospun from polymer dispersion made with 0.691% CNF, 0.01 ml PEGDE and 4 ml PEDOT:PSs per 14 ml of polymer dispersion, applied potential 25 kV, pumping rate 0.6 ml/h. Supporting electrolyte KCl 0.1 M, scan rate 20 mV/s

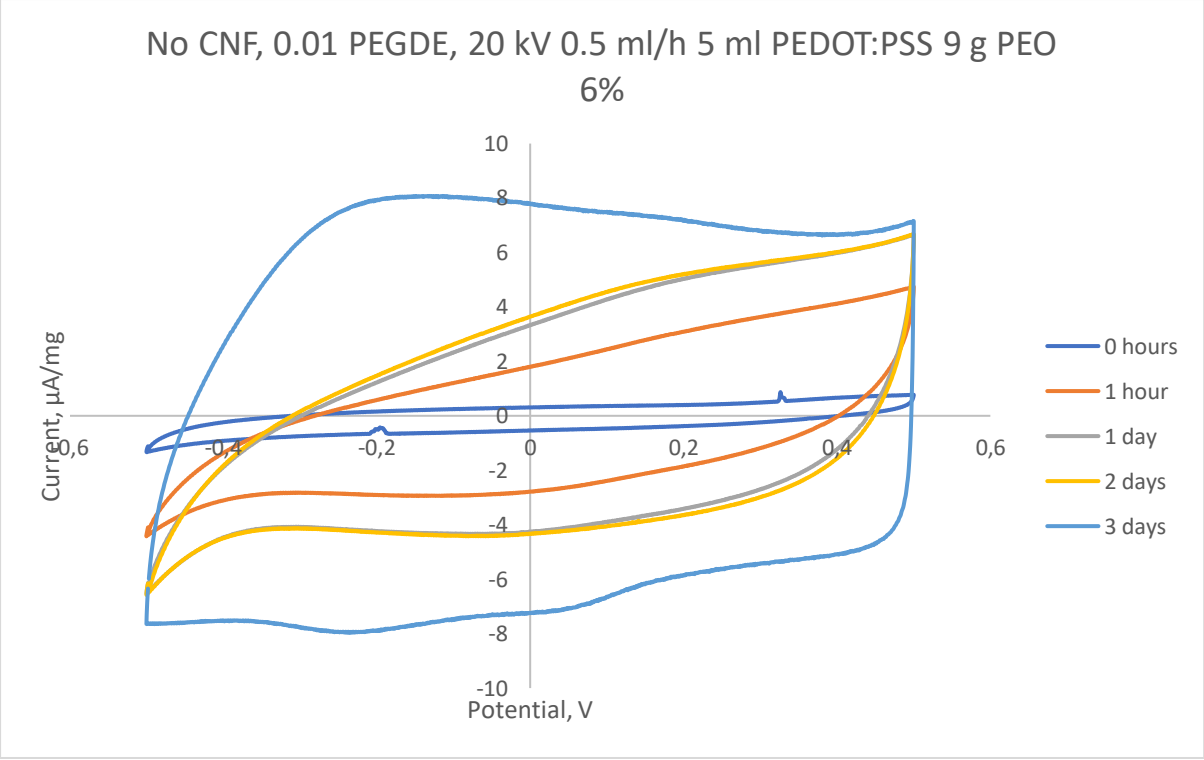

Nanofibers electrospun from polymer dispersion made with no CNF, 9 g of 6wt% PEO, 0.01 ml PEGDE and 5 ml PEDOT:PSS per 14 ml of polymer dispersion, applied potential 20 kV, pumping rate 0.5 ml/h. Supporting electrolyte KCl 0.1 M, scan rate 20 mV/s

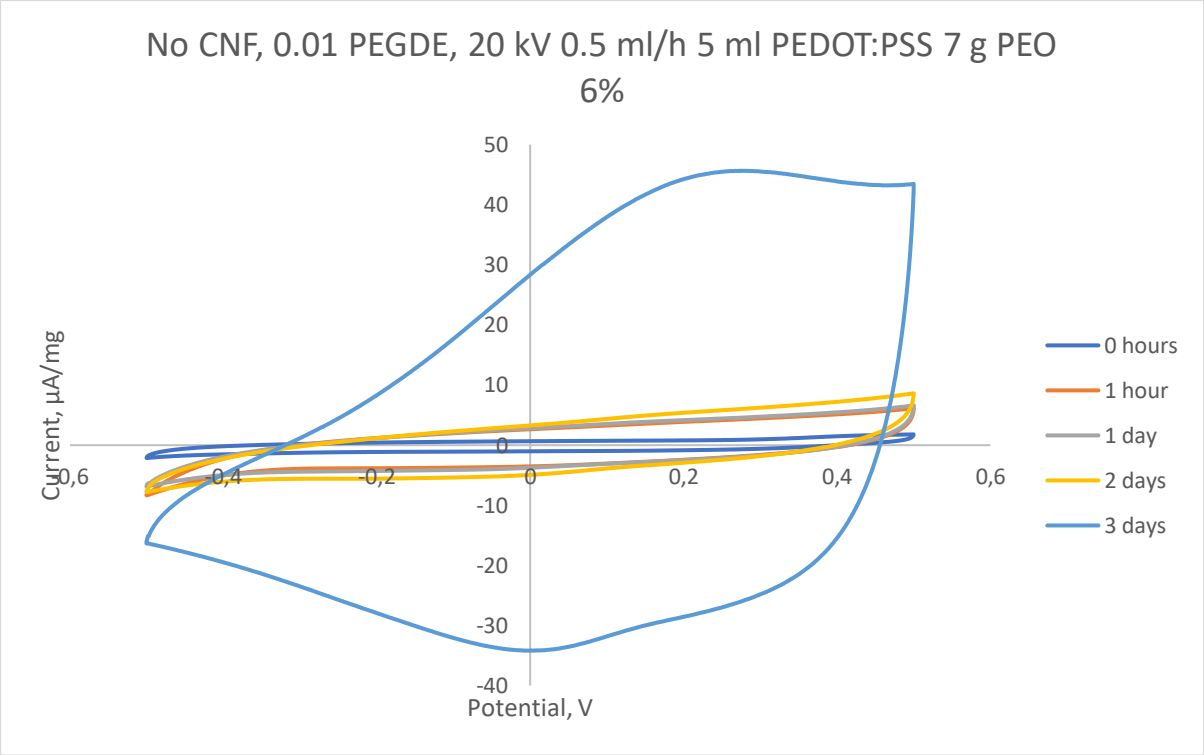

Nanofibers electrospun from polymer dispersion made with no CNF, 7 g of 6wt% PEO, 0.01 ml PEGDE and 5 ml PEDOT:PSS per 14 ml of polymer dispersion, applied potential 20 kV, pumping rate 0.5 ml/h. Supporting electrolyte KCl 0.1 M, scan rate 20 mV/s

7.3. Appendix C
Water contact angle images

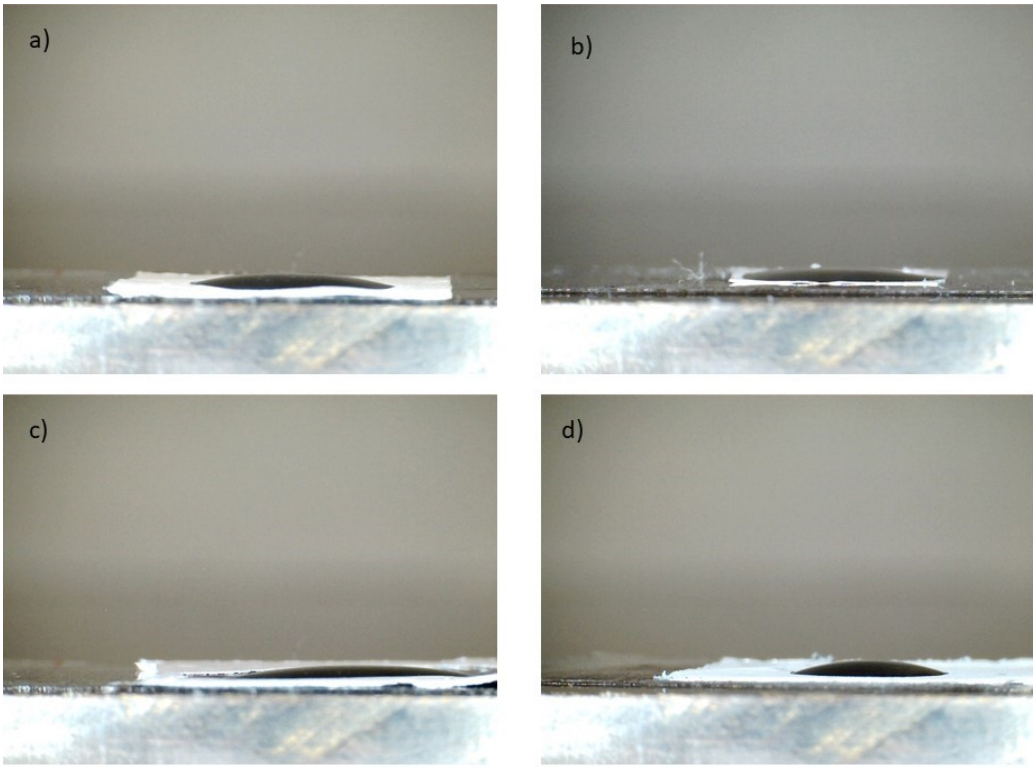

Nanofibers on aluminum foil made with 0.461% CNF, different PEGDE volume and 4 ml PEDOT:PSS per 14 ml of polymer dispersion, applied potential 20 kV, pumping rate 0.5 ml/h a) No PEGDE b) 0.001 ml PEGDE c) 0.005 ml PEGDE d) 0.05 ml PEGDE

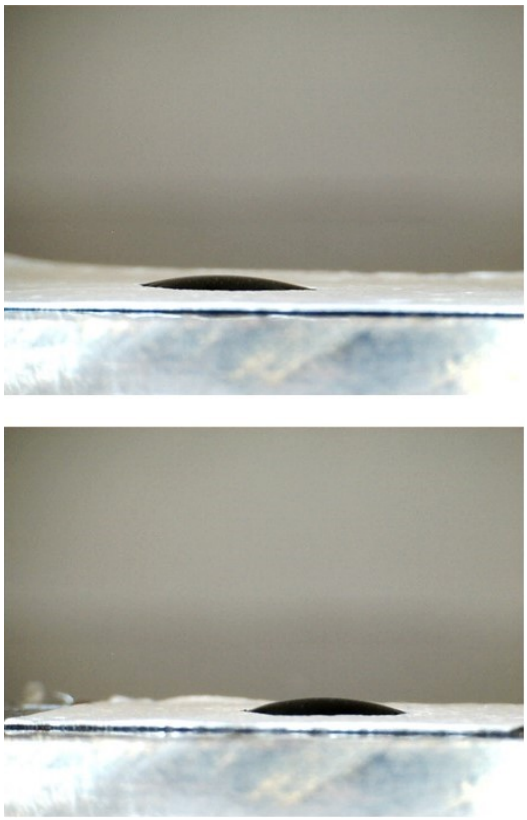

Nanofibers on aluminum foil made with 0.691% CNF, no PEGDE and 4 ml PEDOT:PSS per 14 ml polymer dispersion. Top: Applied potential 20 kV, pumping rate 0.5 ml/h. Bottom: Applied potential 25 kV, pumping rate 25 kV.

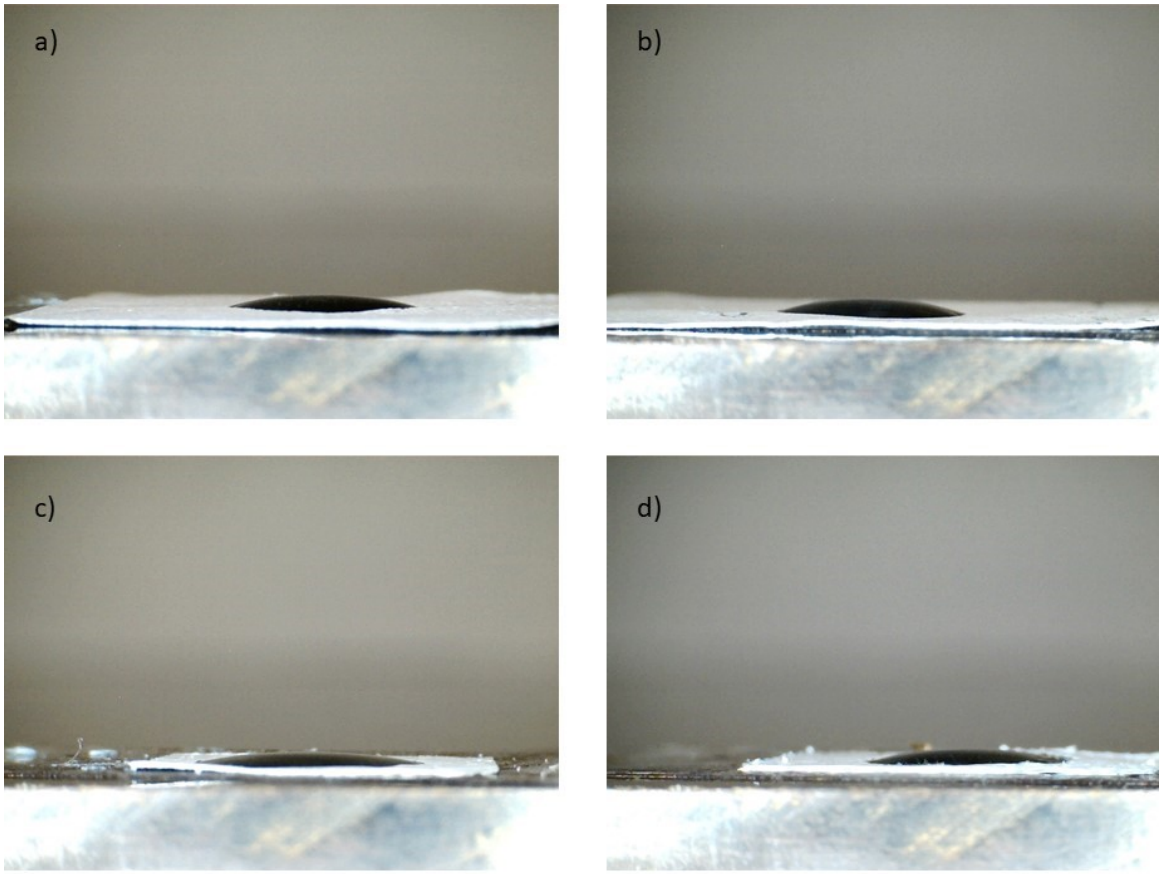

Nanofibers on aluminum foil made with 0.691% CNF, 5 ml PEDOT:PSS per 14 ml of polymer dispersion. Left column: applied potential 20 kV, pumping rate 0.5 ml/h Right column: applied potential 25 kV, pumping rate 0.6 ml/h. Top row: No PEGDE Bottom row: 0.01 ml PEGDE per 14 ml of polymer dispersion